SEDIMENT AND PESTICIDE TRANSPORT PROCESSES WITHIN A SMALL AGRICULTURAL WATERSHED

Thesis for the Degree of M. S.

MICHIGAN STATE UNIVERSITY
ROBERT E. SNOW

1977

ABSTRACT

SEDIMENT AND PESTICIDE TRANSPORT

PROCESSES WITHIN A SMALL AGRICULTURAL WATERSHED

by

Robert E. Snow

The concentration of suspended sediment and pesticides of the chlorinated hydrocarbon group were measured during surface runoff on a small agricultural watershed to determine the transport processes operating in this non-point source problem. Determination of the origin of the wash load and bed material load, along with an evaluation of the hydraulic nature of the stream, result in a basic understanding of the transport processes and provide insight into the problem of predicting sediment and pesticide loads.

By measuring the concentration of the suspended sediment and pesticide as well as the stream discharge during surface runoff, the suspended sediment and pesticide loss from the watershed was calculated. Time signatures of the pesticide concentration, suspended sediment concentration, and stream discharge were superposed in an attempt to identify correlations between these variables.

The effects of overland flow erosion and channel scour were discussed with emphasis on the entrainment of bed particles. An analytical approach was utilized to determine the influence of seepage forces on the bed erosion process. The results suggest that groundwater seepage into the stream may significantly affect the sediment entrainment process. However, because of the complex nature of the flow pattern caused by seepage, it was difficult to estimate the drag and lift forces.

A discussion of the hydrodynamic roughness condition of the stream bed with respect to sediment and pesticide entrainment was presented. A high correlation between stream discharge and pesticide concentration was realized for the conditions of a hydraulically rough bed and insignificant wash load.

SEDIMENT AND PESTICIDE TRANSPORT PROCESSES WITHIN A SMALL AGRICULTURAL WATERSHED

by

Robert E. Snow

A THESIS

Submitted to
Michigan State University
in partial fulfillment of the requirements
for the degree of

MASTER OF SCIENCE

Department of Civil and Sanitary Engineering

1977

ACKNOWLEDGMENTS

The writer wishes to express his sincere appreciation to Dr. Dave A. McIntosh for his guidance and perception during the course of this study. Discussions with Dr. David C. Wiggert were very constructive and his encouragement was gratefully appreciated. Acknowledgment is also extended to Dr. Thomas Burton and Dr. Matthew Zabik for their technical contributions. The writer also wishes to thank Mr. Paul C. Bent for his initiative and skill in carrying out the data acquisition and his assistance in understanding the hydrology of the watershed.

Gratitude is expressed to the Institute of Water Research at Michigan State University and the United States Environmental Protection Agency for support of the project.

The writer is appreciative of the assistance of associates and friends during the completion of this study who have made this experience enjoyable and satisfying.

TABLE OF CONTENTS

LIST OF TABLES

LIST OF FIGURES

Figure		Page

Figure		Page

NOMENCLATURE

A_C	area of contact	L^2
C	flow coefficient	
C_D	drag coefficient	
C_F	form drag coefficient	
C_L	lift coefficient	
d	particle diameter	L
D	dimensionless distance above bottom	
e	porosity	
F_1	force perpendicular to the stream bed	ML/T^2
F_{11}	force parallel to the stream bed	ML/T^2
F_{DF}	form drag force	ML/T^2
F_{DS}	viscous drag force	ML/T^2
F_L	hydrodynamic lift	ML/T^2
F_S	seepage force	ML/T^2
F_{SL}	shear lift force	ML/T^2
$\partial h/\partial y$	piezometric head gradient	
k_s	bed roughness	L
$\partial P/\partial y$	instantaneous pressure gradient	
Q	stream discharge	L /T
Q_S	sediment discharge	M/T
u	free stream velocity	L/T
u_*	shear velocity	L/T

$\bar{U}_T$	time average velocity at top of sphere	L/T
$\bar{U}_{35}$	time average velocity measured .35 grain diameters above the bed plane	L/T
$\bar{u}(y)$	velocity profile	L/T
$\partial V/\partial y$	velocity gradient	
$\bar{V}_o$	time average velocity upstream of particle	L/T
W	particle weight	ML/T^2
W_B	particle bouyant weight	ML/T^2
α	bed slope	
β_1	area proportionality factor	
γ	specific weight of fluid	M/T^2L^2
γ_s	specific weight of the particle	M/T^2L^2
δ	viscous sublayer thickness	L
μ	viscosity	M/LT
ν	kinematic viscosity	L /T
ξ	momentum correction coefficient	
ρ	fluid density	M/L^3

CHAPTER 1

INTRODUCTION

The transport processes, the combined system of pollutant and transporting medium, are a significant part of the erosion and sedimentation of a non-point source pollutant. The natural process of erosion of sediments constitutes a non-point source problem, and with the possibility of pesticide dissolved in the flow as well as adsorbed on particulate matter, the analysis of the transport of sediments can aid in controlling its propagation in the environment.

The rainfall-runoff process is responsible for the transport of soil particles from the land surface to the stream. Once in the stream, the finer solids remain suspended because of their dispersive nature, while larger particles are held in suspension by the motion of the fluid. Particulate matter that settles is collected at the bottom and may remain stationary, move along the stream bed with saltation, or be resuspended during the next storm. Of particular interest is the suspended solids which can directly transport pesticides at high concentration during the runoff of a storm. The material moving along the bottom, the bed load, is a slow transporting process and as a result pesticides can remain in the stream for a longer period. This transporting process is not as serious because the composition of the bed material, large sand particles, is such that it is least active in adsorption of pollutants.

The Mill Creek Pilot Watershed located in midwestern lower Michigan is the site at which this study is being conducted. Fruit orchard watersheds such as Mill Creek receive seasonal pesticide application and fertilization. Preliminary studies carried out in the 1960's indicate that this type of agriculture represents a serious non-point source of pollution to Lake Michigan. Of interest in this study is the identification of suspended sediment and pesticide levels and their relationship in unsteady flow and an investigation into the effect of ground water intrusion through the stream bed.

To facilitate the identification of sediment and pesticide transport relationships, data was taken during surface runoff events. It was anticipated that the pesticide traces would be highly irregular from event to event due to the rainfall distribution and varied agricultural usage. The pesticide p,p'DDT, and to a lesser extent the other chlorinated hydrocarbon pesticides, should be consistent because of its persistence and the fact that it is no longer applied. Suspended sediment should also be consistent with some variations due to seasonal and land use effects.

The pesticides of interest in this study were a group of chlorinated hydrocarbons: p,p'DDT, p,p'DDE, Dieldrin, Aldrin, Lindane, and Heptachlor Epoxide. Concentration determinations were made for both the pesticide dissolved in water and the pesticide adsorbed on particulate matter in the flow. Suspended sediment was analyzed for the concentration transported by the stream and a determination of the grain sizes present. The angle of repose of the bed material was also measured. The relationship between suspended sediment and pesticides was difficult to ascertain because of the nature of a watershed system.

Substantial results or empirical relationships could not be obtained because of lack of data due to an exceptionally dry sampling period (approximately 8 months). However, the event data available has been analyzed and is a start in understanding the process of suspended sediment and pesticide transport.

In the lower portion of the watershed, it was evident that due to a relatively high ground water table, intrusion occurred through the stream bed. In several areas, piping of the sand bed was apparent. As a result, a theoretical analysis is carried out to determine if this ground water seepage has a significant effect in sediment entrainment and transport.

The hydrodynamic forces exerted on the particles located at the stream bed surface can be affected by seepage. The major components of the forces are the shear stress due to particle friction and form drag in the direction of flow. The force normal to the flow is the hydrodynamic lift on the particle.

Because stream bed particles are more likely to be blunt than streamlined, the form drag caused by the pressue distribution over the particle surface is at least as large as the viscous shear on the cohesionless particles. In addition, the hydrodynamic lift is also dependent on the pressure distribution, which is in turn dependent on the flow pattern and velocity around the particle.

Seepage in a permeable bed changes the flow pattern near the bed surface which has a direct effect on the particle boundary layer. If the flow pattern around the particle is altered the pressure distribution on the particle surface and, therefore, the lift and drag forces will be changed. The viscous boundary layer may be increased due to effluent seepage and a hydraulically rough flow, the flow conditions where the bed particles penetrate the viscous boundary layer, may be changed into hydraulically smooth flow with the viscous boundary layer completely enveloping the bed particles.

The literature review highlights investigations involving a detailed consideration of the forces acting on individual particles. However, the nature of these forces as they apply to the in-stream transport process is not fully understood. In spite of this, the literature review serves to alert one to the complexity of this problem. The analysis of sediment transport is further complicated by overland flow erosion, unsteady and nonuniform flow, and channel instability (Chapter 3). In addition, fluid turbulence affects the magnitude and time variation of the hydrodynamic forces on the stream bed (Chapter 4). Although it is necessary to simplify the problem in order to obtain estimates of sediment transport (Chapter 5), interpretation of the results should reflect the complex flow field and the hydrodynamic roughness of the bed.

CHAPTER 2

LITERATURE REVIEW

The freshwater ecosystem has received considerable abuse from the use of pesticides. Surface water contamination is principally caused by agricultural activities, as reported by Li and Flick (1972). In addition to aerial spraying and runoff, careless application practices and disposal or washing of pesticide containers have added substantial amounts of pesticides to surface waters. Berck (1953) observed the presence of DDT and its metabolites in bottom sediments of lakes and streams. The sediment particles resting on the bed are available for suspension and thus represent a source of non-point pollution to surface waters.

The major hydrodynamic forces exerted on particles resting on the stream bottom include the form drag and hydrodynamic lift. By convention, the drag and lift forces have been defined as dependent on the flow velocity and density, and the particle cross sectional area. The forces differ by a coefficient. The coefficient for the drag force is normally dependent on particle shape and flow Reynolds number. The coefficient for lift is usually a function of particle shape and position with respect to the flow. The effect of seepage is to change the flow pattern around the bottom particles having a direct effect on the flow velocity and particle surface pressure distribution. Maintaining the standard definitions for lift and drag require the seepage effect to be incorporated in the lift and drag coefficient.

2.1 Pesticide Studies

Several studies have been conducted on the transport of pesticides in the water environment. Because of the possibility of adsorption of pesticides on soil particles as well as pesticide solubility, two modes of transport are available. Barthel (1966) showed that transport mechanisms for the chlorinate hydrocarbons, the group of pesticides of major interest, is through erosion movement of soil particles. Colloidal size particles are the most effective mechanism because they are most active in adsorption and are readily dispersed and stable in suspension. Shin (1970) outlined chemical reasons for the preferential adsorption of p,p'DDT and other hydrocarbons for small, organic matter.

Smith (1974) investigated pesticide loss from claypan soils, determining the quantity carried in runoff and the most effective farming practice: minimum or no-till row crop production. Further work on the transport and deposition of pesticides was done by Sckacht (1974) who determined concentrations on soil particles and in stream flow. Results indicated that the pesticides heptachlor, heptachlor expoxide, dieldrin, methoxychlor, lindane, aldrin, endrin, and p,p'DDT have limited solubility; the dissolved concentration in the part per trillion range and the adsorbed concentration in the part per billion range.

Sanborn (1974) studied the persistence of pesticides after application. Pesticides of interest in the study include Dieldrin and Lindane. Li and Flick (1972) compiled a list of common pesticides and their persistence time for several different types of soil, finding strong correlation with the chemical character of the pesticide and organic constituents of the soil.

Gillett, Hill, Jarvinen, and Schoor (1974) developed a conceptualized model for the movement of pesticides in the environment. The detailed processes of transport and deposition were used by Donigian and Crawford (1976) to model pesticide transport with some success.

Other studies have been conducted on the local and state levels to determine pesticide runoff and effective control by farm practices. It is difficult to apply the results because of the wide range of pesticides encountered, but particularly because of the dependence on soil type.

2.2 Sediment Entrainment

Entrainment of particles resting on the stream bed is a complex process because of turbulent flow over the bed. The conventional representation of turbulence produced the following flow model. The flow creates a boundary layer near the stream bed which is fluctuating, but is represented at a mean distance from the bottom. Because of the no-slip condition at the bottom, the turbulent flow in the boundary layer must come to rest at the boundary. To do this, the flow velocity near the boundary must decrease according to some gradient. At some point in depth above the bottom, the velocity is such that the flow may be classified as laminar. At this point the laminar or viscous sublayer begins and extends to the stream bed.

2.2.1 Turbulence

Pick-up due to turbulent fluctuations, whether in the form of velocities or forces, has been confirmed as a significant though unweidly factor in the initiation of sediment movement. The conventional description of the turbulent boundary layer including a viscous sublayer is not entirely accurate. From flow visualizations, it has been observed that the random effects of turbulence cause the viscous sublayer to fluctuate and at times disappear. Brodkey (1977) proposed that the disruption of the apparent viscous sublayer is cyclic rather than random. From flow visualizations, he followed the path of fluid particles within the viscous boundary layer by injecting neutrally bouyant visible particles. A cycle was defined in which a deceleration of flow along the wall was followed by accelerated bursts of fluid in a trajectory towards the wall at some acute angle with the free stream. This resulted in a sweeping motion along the wall until deceleration was again observed. This is similar to the theory of random turbulent bursts which destroy the viscous sublayer.

Einstein and Li (1958) studied the intermittency of the laminar sublayer and Sutherland (1967) made simultaneous observations of entrainment of sediment grains and disruptions of lines of dyed fluid along the bed. Turbulent bursts of high velocity fluid from the flow impinge on the bed, temporarily disrupting the viscous sublayer and creating a pulse intense enough to set grains in motion. The pulse must be of the magnitude of the resisting force, the weight of the particle. Yalin (1972) further investigated the lifting of particles in terms of turbulent eddy motion.

Kalinske (1947) investigated the instantaneous shear stress applied to the bed by considering the turbulent velocity fluctuations. He indicates that instantaneous shear can exceed the average by a factor of three. Gessler (1965) proceeded along the same path, computing the probability of grain erosion. Yalin (1963) pursued the turbulent velocity fluctuation effect on critical shear with an analytical approach. From laboratory observations, Raudkivi (1963) showed that sediment entrainment is a function of the temporal mean drag on the bed and the turbulence of flow over it.

The conventional representation of turbulent flow can be readily used in analysis of forces on bed particles whereas the actual flow pattern is too complex. Theoretical and laboratory work has been undertaken to define the critical condition for sediment movement on mobile beds. The descriptive approach investigators have taken to determine the critical conditions fall into three categories: pick-up velocity concept, drag force concept, and lift force concept.

2.2.2 Pick-up Velocity Concept

The pick-up velocity concept was first suggested when Brahms (1753) published a sixth power law for incipient motion. The sixth power law is a relation in which the critical velocity, the flow velocity at which particles are entrained in the flow, is proportional to the weight of the particle to the one-sixth power. Several investigators developed critical velocity relationships dependent on particle characteristics, but Rubey (1948) found that these laws only applied when the dimensions of the particle are large compared with the thickness of the laminar sublayer for turbulent flow. White (1940), Shields (1936), and Tisen (1953) did further work which confirmed this result. Sternberg (1875) obtained very good results by combining the sixth power law with a particle movement relationship of exponential form. Data from field and laboratory observations has been tabulated for several materials by Fortier and Scibey (1926).

While a critical velocity may still be used in design of stable channels, it is an outdated concept for explaining the initiation of sediment motion. Mavis and Laushey (1948) attempted to determine critical velocity by the stability equation with the inclusion of drag. Ippen (1953) included both drag and lift forces in his development of a critical velocity relationship with some success.

2.2.3 Drag Force Concept

The drag force as the critical parameter for incipient motion was first investigated by Schoklitsch (1914). His development considered the tractive shear as a function of particle weight. Krey (1921) and Kramer (1935) expanded Schoklitsch's analysis to include bed properties rather than just particle characteristics. Application of Kramer's relationship for critical shear was successfully done by O'Brien and Rindlaub (1934). A different approach was taken by Chang (1939) who performed a dimensional analysis and Meyer Peter and Muller (1948) who derived the critical tractive force from a bed load formula. Shields (1936) introducted into the analysis of the drag concept the dependence of shear on the boundary or shear Reynolds number, a widely accepted relationship. The shear Reynolds number is similar to the flow Reynolds number in which the shear velocity, the shear stress divided by the fluid density to the one half power, is substituted for the flow velocity and the particle is the important unit of length. White (1940) provided data for a critical drag force relationship, the tractive force required to entrain particles, involving the positioning of particles in the bed. Egiazaroff (1957) developed the critical shear stress theory from combining critical velocity and drag which agrees qualitatively with Shields and White.

Chepil (1959) introduced a threshold relationship which included the lift force measured experimentally. The lift force was empirically related to the drag and a relation for critical drag and shear was developed dependent on the particle positioning on the bed.

2.2.4 Lift Force Concept

Jeffreys (1929) was the first to show that classical hydrodynamics provides a possible explanation for entrainment of particles by a lift force due to potential flow over the surface. Reitz (1936) further developed the lift model using circulation and viscosity. Measurements of lift on sediment in a bed were made by Einstein and El Samni (1949) and Apperley (1968). Apperley's investigation indicated the lift forces on bottom particles are predominantly negative, depending on the distance from the bed, but that there were infrequent bursts of large positive lift forces indicating the role of turbulence. Lane (1936) and Kalinske (1942) stressed the role of turbulence in the determination of lift forces. Yalin (1963) presented photographic evidence that particles, in some conditions leave their position in a vertical upward direction rather than being rolled out of position about some point of contact. The lifting mechanism is represented as the energy required to lift the bouyant weight of the particle one particle diameter. In turbulent flow, the energy required to lift the particle is obtained from vortex shedding off of upstream grains which cause non-uniform pressure and velocity distribution.

2.2.5 Drag and Lift

The lift and drag force concept has been recently considered by many investigators as the critical parameters for initiation of motion. Coleman (1967) contributed a theoretical and experimental study of drag and lift forces. For a hypothetical stream bed, he introduced a critical force function dependent on drag and lift, where lift was defined as directly proportional to the particle weight. The conventional definition for the drag was used, dependent on the flow velocity. Hydraulically smooth to rough conditions were investigated yielding results in terms of the fluid driving force and Reynolds number. The direction of the lift force was ascertained; the point of zero lift effect occurs when the laminar sublayer is approximately equal to the bed roughness. The lift force is negative for a larger laminar sublayer and positive for the hydraulically rough condition. The drag coefficient for the fluid driving force agrees with free fall predictions and lift proportionality factor was determined for the range of Reynolds numbers. These results agree with the work done by Apperley (1968).

Aksoy (1973), using the force relationship dependent on uniform velocity, defined lift and drag coefficients over a limited range of Reynolds numbers for the hydraulically rough situation. The drag coefficient for the drag force agrees reasonably well with work done by Garde and Sethuraman (1969) for spheres rolling down an inclined plane. An explanation of the difference in drag coefficients in Aksoy's and Coleman's work is that Coleman's fluid driving force includes the effects of both drag and lift. In Aksoy's work the lift forces were relatively small, approximately one-seventh of the drag force.

Nonuniform velocity profiles were taken into consideration by Chen and Carstens (1973) by means of a momentum correction coefficient in a single velocity dependent force relationship for lift and drag. Moments rather than forces were used in the analysis of a sphere-pin system. The ratio of lift to drag was found to decrease from 1.6 to .4 as the protrusion of the particles in the bed increased from 25 to

100 percent. This differs from the one-seventh ratio Aksoy determined for his 100 percent protrusion case because of the inclusion of the momentum correction coefficient and exceptionally high velocities in Chen and Carstens procedure.

Tarimcioglu (1973) introduced a function for lift involving the free fall velocity of a particle rather than the flow velocity in his analysis of critical conditions. A critical relationship was defined for lift, velocity, friction, depth, energy gradient, and free surface slope from the study of a single layer of spheres forming the bed. From the analytical study, the critical condition for entrainment was determined to be when the maximum fluctuating lift force reached the particle bouyant weight. This result along with the critical condition for velocity can be used to calculate the lift coefficient dependent on particle size. The values obtained agree fairly well with data taken by Aksoy.

2.2.6 Seepage

In addition to the fluid dynamic lift force, another lifting force can exist as a result of seepage through the stream bed. Clayton, Tuthill, and Bickley (1966) observed that groundwater seepage out of the bed and into the flow of an Alaskan stream increased sediment transport by a factor of 1000. In contrast, Harrison (1968) conducted experiments which indicated that seepage had no effect on incipient motion and sediment transport. Martin's (1970) study on seepage as it affects boundary layer characteristics of the flow, as well as resultant forces, produced evidence in agreement with Harrison, i.e., seepage out of the bed does not appear to affect incipient motion even up to a fluidized or quick condition. However, the study involved an oscillating water surface in which the time average flow over the bed was zero. Martin (1971) determined from an experimental study that the seepage force on the top grains is approximately .35 to .40 times that on grains well into the bed because fluid resistance is greater due to surrounding bed particles. When the fluidized bed condition develops with stronger seepage forces at the bottom layers of the bed, piping effects result in considerable particle uplift in the flow.

Watters and Rao (1971) conducted experiments to determine the lift and drag forces under seepage conditions for a series of bed configurations. The flow was in the transition zone between hydraulically rough and smooth conditions. Unlike Martin's (1970) experiment, Watters and Rao set up flow over the bed. Their results indicated that effluent seepage decreased drag regardless of the bed configuration. The lift, empirically found to be in the direction of the bed for all seepage conditions investigated, decreased in magnitude due to effluent seepage and increased in magnitude with influent seepage for a plane bed (angle of repose $\phi = 90°$). For particles above the bed plane (angle repose $\phi = 60°$), the magnitude of the lift increased for effluent seepage and decreased for influent seepage. In other words, for this bed condition upward seepage through the bed caused an increase in force toward the bed. In agreement with previous investigators, the lift and drag forces are of comparable magnitude and both should be considered in a stability criterion.

The experiments by Martin (1970) and Watters and Rao (1971) indicate that the direct effect of effluent seepage is to rock the particle out of its recess, but the boundary layer alteration results in reduced drag. For a bed condition similar to streams (angle of repose $\phi = 60°$), the magnitude of the lift force is increased. Watters and Rao found that for a high seepage velocity (1 fps), the drag is reduced by half and the lift magnitude increased by thirty percent. Therefore, effluent seepage may have a significant effect on entrainment. This is contradictory to Martin's conclusions, a result of his experimental setup.

The literature indicates the importance of lift and drag forces on the stability of a bed particle. No information is available concerning seepage flows in the hydraulically smooth condition, the flow condition of Mill Creek. If the results of Watters and Rao's (1971) experiment can be extended to this flow region, then effluent seepage could be expected to inhibit entrainment. However, it should be recognized that turbulent fluctuations play an important role in entraining particles which under statistically average conditions should remain at rest.

CHAPTER 3

AN OVERVIEW OF SEDIMENT AND PESTICIDE TRANSPORT

The movement of soil particles from their original position on the land surface is dependent on several factors and can follow a variety of routes. The adsorption and dilution of pesticides in the sediment-laden runoff adds to the complexity of pesticide transport. The obvious relation of sediment to pesticide adsorbed on the soil particles indicates the importance of understanding sediment erosion and transport.

3.1 Pesticides

Once pesticide is applied, it begins a chemical interaction with soil particles. With the occurrence of overland flow, it may be transported in either of two forms: (1) adsorbed on sediment particles and (2) in solution. Movement is quite dependent on sediment transport in that the pesticides of interest, the chlorinated hydrocarbon group, is practically insoluble. The water solubility limits for this group range from 11 to 110 ppb (Sckacht, 1974).

Soil type may be the most important parameter affecting the adsorption of pesticides on soil. Adsorption is dependent on soil properties such as organic content, clay content, ion-exchange capacity, surface area, and pH. Persistence of a pesticide generally increases with an increase in organic material and with increase in clay content. The longer persistence is due to increased adsorption of the pesticide onto the organic and clay particles, thus decreasing the availability of the pesticide for microbial decomposition, volatility, and leaching.

Pesticides which reach a watercourse are liable to be transformed into other chemicals:biologically by sediment and water microorganisms, photolysis, or by chemical means. The persistence, toxicity and other physiochemical properties can be affected by these transformations

The persistence of the chlorinated hydrocarbon group varies according to pesticide and soil type. The breakdown of chlorinated hydrocarbons is not exponential, though the term half life is often applied. Actually, the breakdown curve is made up of several distinct components which differ in importance with the climate, season, and soil. Half lives greater than four years are uncommon. The maximum accumulation for a four year half life is about six times the annual dosage (Sanborn, 1974).

The chemical structure of a pesticide is also a factor in its persistence. The nonpolar characteristic of the chlorinated hydrocarbons explain their estimated persistence of from five to thirty years (Shin, 1970).

Persistence of a pesticide is usually different in water than in soil. Pesticides dissolved in water have high freedom of movement and mixing. When a pesticide is transported in water, most of it becomes adsorbed on sediments. After adsorption, a small fraction is gradually desorbed and released into solution. In a quiescent medium, dynamic equilibrium is maintained (Barthel, 1966).

The chlorinated hydrocarbon pesticides of interest are Aldrin, Dieldrin, DDT, DDE, Lindane, and H. Epoxide. Aldrin was introduced about twenty years ago as an effective insecticide for the control of soil insects, particularly those associated with corn. Dieldrin, the the oxidized form of aldrin, is very persistent with a soil half life of about three years. The persistence is related to the extreme inertness toward chemical or biological modification (Sanborn, 1974).

One of the major breakdown products of p,p'DDT is DDE, both of which have been found in significant quantities ten years after application. The quantities found are a function of the particular environment. In soils of high organic content, up to thirty percent of the p,p'DDT applied may remain after ten years. In general, it appears that p,p'DDT degrades more rapidly where a large and varied soil microbe population is present. Lindane and H. Epoxide have persistence times of equal magnitude as the rest of the chlorinated hydrocarbons. It should be recognized that these chlorinated hydrocarbons have not been used for several years and the presence of these pesticides are directly dependent on their persistence (Sanborn, 1974).

3.2 Erosion and Transport of Sediment and Pesticides

With the occurrence of a rain storm, the process of erosion and sediment transport is enhanced. Due to soil splash from rain drops and overland flow, soil particles are eroded and carried to the stream. Pesticides, from recent applications or metabolites from past applications, are available for transport dissolved in solution or adsorbed on soil particles. The increased flow due to surface runoff causes erosion of stream bed particles. This source of soil particles is not as significant with respect to pesticide transport because of preferred adsorption on smaller organic solids. After peaking of the flow, the transport capacity of the stream decreases and deposition results. The particles first deposited are ordinarily the larger grains originating from bed or bank erosion and, therefore, may not be significant in pesticide transport. The small organic material is usually held in suspension during the hydrograph recession and, hence, contribute to the pesticide yield of the watershed.

Erosion is a process dependent on local conditions. As a result, a particle of soil may take a considerable amount of time to move out of the watershed. The transport of pesticide on suspended matter is not only dependent on sediment transport, there are sources and sinks within the process. Pesticides adsorbed on the particles are subject to chemical action and degradation. In addition, the possibility of adsorption and desorption between the soil particles and the flow exists.

3.2.1 Erosion

There are two categories of erosion: sheet erosion and channel erosion. Sheet erosion is the somewhat uniform removal of soil from the land surface without development of definite channels, although small rills caused by localized concentration of flow are included in this category. This kind of erosion is the product of raindrop impact combined with overland flow. Raindrop impact breaks down soil aggregates and splashes soil particles into the air. When overland flow is present, the splashed particles fall into sheet flow and are transported toward the stream.

The transporting medium induces channel erosion. Channel erosion is the removal of soil by the flow itself. Stream bank and bed erosion, valley trenching and gulley formation constitute the main forms of channel erosion.

The fine sediments are mainly contributed by sheet erosion and coarse particles are supplied by channel erosion. Pesticide movement is more likely to be initiated by sheet erosion, but in orchard areas, it is not uncommon for gulleys to form in areas of application.

3.2.2 Transport

The sediment in transit is usually divided into two components: wash load and bed material load. The wash load consists for the most part, of fine material which is swept in suspension through the channel reach. On the other hand, bed-material load usually consists of larger, heavier material which is predominantly found in the stream bed. The bed-material load occassionally goes into suspension, but usually moves by rolling and jumping along the stream bottom.

The basic modes of sediment transport by water are classified as bed load, consisting of the bed-material load, and the suspended load, which is made up of the wash load and possibly a portion of the bed-material load, depending on the flow conditions. Bed load movement is accomplished by rolling, sliding and saltation of the bed material due to the hydrodynamic forces. Particle suspension is the result of the hydrodynamic forces. The concentration of suspended sediment in a stream cross-section decreases with distance from the bottom. The fine particles tend to be dispersed more or less uniformly while the coarse particles provide the concentration gradient.

The transport of sediment load is not a continuous process. Soil particles may come out of suspension or scour may entrain sediment depending on the flow condition. The bottom characteristics as well as flow parameters affect the bed load. Though the sediment load may remain relatively stable during base flow, occurrence of a surface runoff changes the flow and has direct impact on the suspended and bed load.

3.3 Unsteady Flow Effects

Since the flow of natural streams is unsteady, it is to be expected that scouring and deposition will occur. Due to a rain storm, increased flow is routed into the stream along with newly eroded sediments. Channel erosion is encountered and combined with the wash load of the stream. Because of the increase of sediment concentration in the stream during runoff, it is obvious that the erosion and scour process dominates the dilution effect due to the added volume of water.

As the rate of runoff peaks and finally decreases, a corresponding effect on the flow and sediment is observed. The recession of the hydrograph is combined with a faster recession of the suspended sediment concentration. That is, for the same flow experienced during the rising and falling limb of a hydrograph, the sediment concentration will be greater for the rising limb than that of the recession side. This is referred to as the hysteresis effect. The cause of the hysteresis effect lies in the antecedant moisture condition and the availability of sediment as well as flow parameter variations during unsteady flow.

Flow parameter variation includes the hysteresis effect on velocity and depth. These are significant parameters in sediment transport, but do not provide full explanation of the sediment hysteresis effect. After the initial erosion and overland flow of a storm, the soil availability is reduced. The presence of moisture increases the weight of particles available for sheet erosion and in addition creates an adhesive force which helps hold particles in place on the land surface. The antecedant moisture of a watershed is responsible for this effect and gives a good indication of the availability of sediment for transport.

Since pesticide transport is dependent on sediment transport, the pesticide concentrations on adsorbed sediment experience the hysteresis effect as well. Though this effect has been observed, it is apparent that hysteresis of pesticide is not only the result of sediment hysteresis, but is dependent on pesticide degradation, sediment adsorption, and chemical action. These effects cannot be determined until the rates of these processes are established.

3.4 Localized Effects

Included in localized effects are watershed factors which cause fluctuation of discharge, suspended sediment, and pesticide at a particular location. The unsteady nature of streams, with tributary flow and ground water input, has a direct effect on sediment load. The stream flow is defined as nonuniform in that discharge increases in the downstream direction. But in addition, at one location discharge may be unsteady during non-event periods due to a change in the contribution from tributaries and ground water sources. As a result fluctuation in the sediment load is observed. During events, this type of localized effect may result from non-uniform rainfall distribution or isolated storms.

Variation of sediment and pesticide loads during events are not always explained by the hydrograph and hysteresis effect. Sudden influx of sediment due to gulley bank instability can create fluctuations in the pesticide and sediment concentrations. A plug load of this type may be dispersed quickly during high flow or remain relatively unaltered during low flow. Therefore, the concentration time traces for sediment or pesticide may form a continuous curve for high flow hydrographs while fluctuations may occur for a low flow hydrograph.

3.5 Sediment Yield

Measurement of suspended sediment concentration at the mouth of the watershed allows the calculation of the sediment yield of the catchment. The sediment yield is the amount of sediment passing out of the watershed for a particular period of record. Ideally, the sediment yield should include the bed load as well as the suspended load. Records of sediment discharge, the sediment transport rate, published in the United States Geological Survey Water-Supply Papers have been limited largely to information on the suspended load and used in calculation of sediment yield. Procedures are avialable for applying a bed load correction, but no simple rule or formula has been found to be universal. The standard procedure has been outlined by the United States Bureau of Reclamation and is a relation between bed-material discharge per foot of stream width and mean water velocity, or a relation between stream power and shear stress. For streams of small size, this correction may be neglected (Colby, 1957).

Generally, a relationship between suspended-sediment discharge and flow discharge is developed for a sediment station, usually the mouth of the watershed. A plot of suspended sediment discharge versus flow discharge on logarithmic scales is called a sediment transport curve and enables the calculation of suspended sediment discharge for periods when only flow discharge records are available. Sediment yield can thus be estimated using this relationship. This relationship which does not account for the sediment hysteresis effect is best applied for time periods of days to months.

CHAPTER 4

EVALUATION OF FORCES ON BOTTOM PARTICLES AND THE INFLUENCE OF TURBULENCE

The flow of fluid over a flat surface of loose grains can create a condition of bed instability leading to channel erosion. With increasing flow a point is reached when the hydrodynamic forces exerted by the fluid flow are equal to resisting force of the particle and motion is incipient. The actual sediment grains in the bed surface are irregular in shape, size, and angle of repose. An analytical study of the forces acting on the grains is complex such that no generalized approach is adequate. To better understand the forces and their contribution to the entrainment of grains, a spherical form is considered in the analysis of a bed of noncohesive grains.

The model chosen to represent the physical process should simulate the flow conditions but be general enough to develop incipient motion theory. Particle shape is usually generalized as a sphere to facilitate computation of the fluid forces, but special attention must be given to flow conditions. Gradually varied, unsteady, favorable pressure gradient flow with nonuniform velocity and the possibility of the turbulent bursts impinging on the bed particles should be considered for a thorough analysis. The effects of seepage through the bed on the surrounding flow regime must also be taken into account.

4.1 Resultant Force Concept

The conventional approach taken in the analysis of non-cohesive particles is the resultant force concept in which all the forces acting on a bed particle are considered. The investigation of the resisting and entraining forces on an individual particle must include the effects of the overall bed. Figure 1 shows the conceptualized two dimensional bed of particles with roughness k_s, angle of repose ϕ, and particle diameter d. Other relevent properties are the porosity e, specific weight γ_s and the bed slope α. The flow condition of interest occurs at the bed terminus where the location of the boundary layer creates either a hydraulically smooth condition - viscous sublayer is larger than the particle protrudances, or hydraulically rough condition - the protrudances project through the viscous sublayer.

Figure 2 shows the resisting and entraining forces on an individual particle. The resisting force is the bouyant weight, W_B. The entraining forces are the viscous drag, F_{DS}, the form drag, F_{DF}, the shear lift, F_{SL}, the hydrodynamic lift, F_L, and the effluent seepage force, F_S.

4.1.1 Resisting Force

The weight of the particle is a significant resisting force. For a spherical particle, the weight is:

$$W = \frac{1}{6} \pi \gamma_S \, d^2 \qquad (1)$$

The friction due to particle contact is a resisting force occurring as a result of particle bed contact as well as particle contact after entrainment. Effluent seepage flow helps to separate particles on the bed so that particle contact is at a minimum, allowing entrainment without

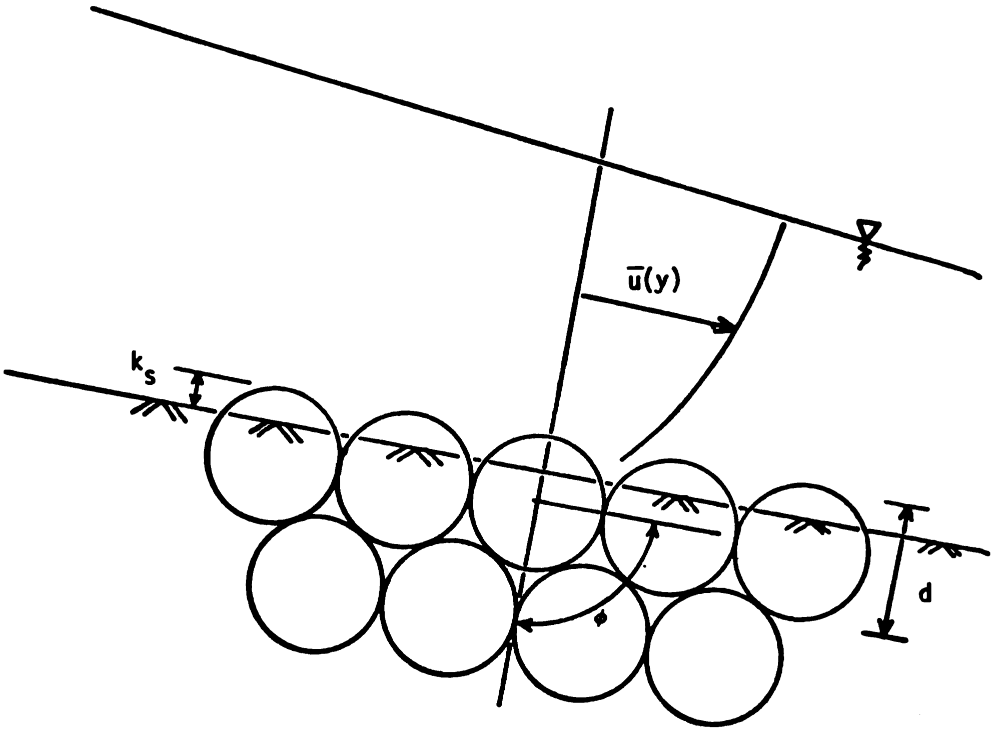

Figure 1. Two Dimensional Bed of Particles

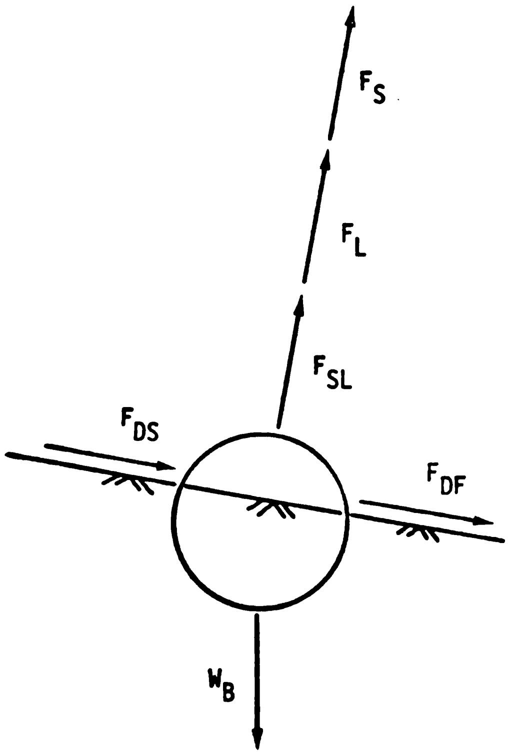

Figure 2. Resisting and Entraining Forces on a Bed Particle the resisting effect of this friction force.

The seepage force due to flow from the stream through the bed does not create a significant force in itself, but does change the boundary layer characteristics. As a result, drag and lift may be reduced and, hence, influent seepage may inhibit entrainment. In addition, in areas of fine silt and clay influent seepage can cause a cementing effect of these fine particles on a sandy bottom.

4.1.2 Entraining Forces

The entraining forces are divided into two groups: hydrostatic and hydrodynamic forces. The hydrostatic force is due to the bouyant pressure on the sphere and is combined with the particle weight to obtain the bouyant weight:

$$W_B = \frac{\pi}{6} (\gamma_S - \gamma) d^3 \tag{2}$$

The hydrodynamic forces include the drag, lift, and seepage and are dependent on the flow conditions as well as the particle characteristics. In addition, seepage has a direct effect on the magnitude of lift and drag because its occurrence alters the viscous boundary layer.

The drag force is the hydrodynamic force parallel to the flow due to the hydrodynamic pressure distribution and consists of two components: viscous drag and form drag. The area of the particle over which the drag acts may not be the entire particle cross-sectional area. As a result, the area of contact is given by the following equation:

$$A_C = \beta_1 \pi d^2 \tag{3}$$

where β_1 is the constant of proportionality.

The viscous drag is:

$$F_{DS} = \beta_1 \pi d^2 \tau_o \quad (4)$$

and acts in the direction of the flow. By definition, the shear stress, τ_o, is dependent on the viscosity and velocity gradient. Due to the presence of other particles on the bed, the shear stress will not be constant over the bed or an individual particle. Therefore, it is difficult to define the viscous drag in this form.

The form drag is due to the hydrodynamic pressure difference around the particle caused by its form and is parallel and in the direction of the flow. Form drag is expressed in terms of the velocity and area of contact:

$$F_{DF} = C_F A_C \rho \frac{\overline{V}_o^2}{2} \quad (5)$$

where $\overline{V}_o$ is the velocity just upstream of the particle. Like the viscous drag, the area of contact is proportional to the cross-sectional area. C_F is the form drag coefficient and is dependent on the flow conditions. The form drag is only significant when separation occurs on blunt bodies, usually at high flow Reynolds numbers. The coefficient must be determined experimentally by measuring the pressure distribution over the sphere and integrating over the frontal area.

The flow conditions dictate the relative importance of viscous and form drag. For Reynolds numbers $(\frac{\overline{V}_o d}{\nu})$ less than 5, the laminar boundary is several grain diameters thick. The flow does not separate behind the individual grains and the drag is due primarily to the viscous shear component. As for flow changes from hydraulically smooth to the transition zone, at a Reynolds number of 10, flow separation occurs and the form drag increases to about one half of the total drag. At a

Reynolds number of 70, the laminar sublayer is interrupted by the existing bed roughness of the grains and the hydraulically rough condition occurs. The turbulent boundary layer is reduced in thickness and the rough boundary creates a source of turbulence. The influence of viscosity is insignificant and the drag is mainly form drag dependent on velocity.

To simplify the dependence of the drag on the flow conditions, the viscous and form drag are usually combined into one expression dependent on velocity and particle area. The flow condition enters the equation in terms of a drag coefficient, C_D, which is a function of the Reynolds number. Due to the presence of non-uniform velocity and interference of upstream particles, another coefficient, ξ, was introduced by Chen and Carstens (1971) into the drag equation:

$$F_D = C_D \; \xi \; A_C \; \rho \frac{\overline{U}_T^{\,2}}{2} \tag{6}$$

where $\overline{U}_T$ is the time average velocity at the top of the sphere, ξ is the momentum correction coefficient, and C_D is the drag coefficient.

The lift force is the force perpendicular to the flow and has two components: a hydrodynamic force due to the hydrodynamic pressure distribution and the vertical component of the viscous drag. As the fluid passes the particle, the streamlines are deflected as shown in Figure 3. Due to the flow over the upper surface of the particle, the pressure is reduced whereas underneath the particle, where the intersticial velocity is relatively small, the pressure is basicly static. As a result of the pressure difference, the hydrodynamic lift force is given by the following relation:

$$F_L = A_C \; C_L \; \rho \frac{\overline{U}_{35}^{\,2}}{2} \tag{7}$$

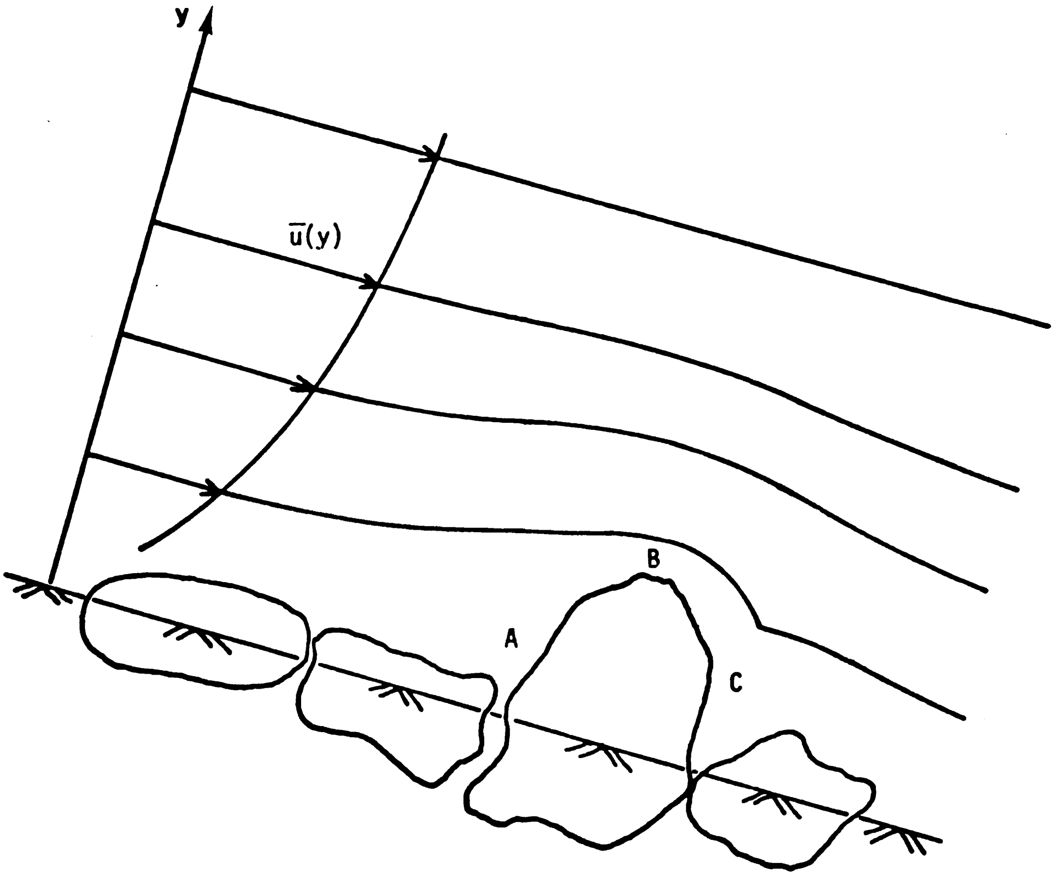

Figure 3. Flow Adjacent to a Bed Particle

where $\overline{U}_{35}$ is the temporal mean velocity measured .35 grain diameters from the bed plane (Einstein and El Samni, 1949).

As already discussed in relation to drag, the viscous shear exerts a shear force over the bed particle. The viscous drag is composed of the shear component parallel to the flow. There exists a shear component perpendicular to flow, called shear lift, due to the geometry of the particle. Figure 4 shows the resultant shear force vectors on a hemisphere on the bottom experiencing flow separation. By integrating the vertical shear component over the surface of a hemisphere, the shear lift can be calculated:

$$F_{SL} = \frac{\pi d^2}{8} \mu \frac{\partial V}{\partial y} \tag{8}$$

where μ is the viscosity of the fluid and $\partial V/\partial y$ is the velocity gradient. This force is normally very small compared with the hydrodynamic lift. For the conventional description of turbulent flow with a laminar sublayer, it is insignificant. However, it is possible for the instantaneous velocity gradient to be quite large due to turbulent bursts penetrating the sublayer. This may create significant shear lift and in combination with the hydrodynamic lift may entrain bed particles.

The seepage force is the hydrodynamic force perpendicular to the flow as a result of fluid flow through the bed. It can be either a resisting or entraining force, depending on either influent or effluent seepage, respectively. The seepage force is usually not represented in terms of flow parameters because normal seepage velocities are much smaller than stream velocities. From porous media flow theory, the seepage is dependent on the piezometric head gradient. The seepage force on the interfacial bed particles is less than that predicted by

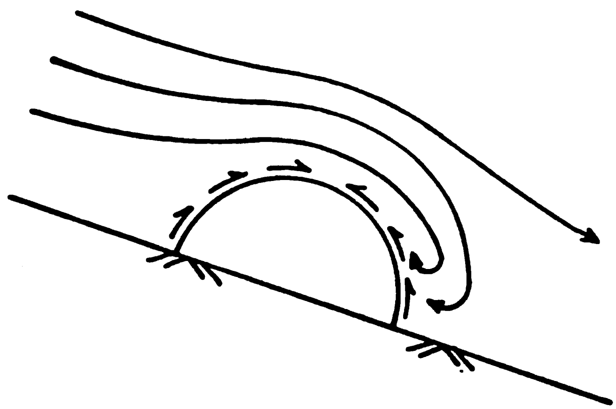

Figure 4. Resultant Shear Force on a Hemisphere

theory because the flow pattern within the intersticies on the top layer is different from that on particles within the bed. McNown (1967) showed that in laminar flow through various curved passages, the total viscous resistance and, therefore, seepage force occurs at the location of minimum pore area. This indicates that the particles deep within the bed experience a larger force than those at the bed terminus. Martin (1971) took this into account when he defined the seepage force per unit volume of sediment as

$$F_{SV} = C\ \gamma\left[\frac{\partial h}{\partial y}\right]_{bed} \tag{9}$$

where C is the flow coefficient dependent upon the shape and packing of the bed particles and $\partial h/\partial y$ is the piezometric head gradient. The seepage force on a bed particle may be calculated by the following equation:

$$F_S = C(1+e)\ \gamma\ \left[\frac{\partial h}{\partial y}\right]_{bed} \frac{\pi d^3}{6} \tag{10}$$

4.2 Incipient Motion Criterion

An incipient motion criterion can be formulated with the resultant force concept. If the forces in Figure 6 are resolved into a component parallel and one perpendicular to the bed, the point of incipient motion occurs when the following equation is satisfied:

$$\tan\phi = \frac{-\Sigma\ F_{11}}{\Sigma\ F_1} \tag{11}$$

where ϕ is the natural angle of repose, ΣF_{11} is the sum of the forces parallel to the bed, and ΣF_1 is the sum of the perpendicular forces. Substituting the relations for the forces into the incipient motion equation and reducing, the following equation is obtained:

$$\tan\phi = -\left[\frac{F_D + W_B \sin\alpha}{F_L + F_{SL} + F_S - W_B \cos\alpha}\right] \tag{12}$$

where α is the slope of the bed.

Typical values of the angle of repose, ϕ, indicate that at the point of incipient motion, the ratio of parallel to perpendicular forces vary from .4 to 1.6. This indicates the importance of the bed configuration with regard to which forces dominate.

4.3 Analysis of Incipient Motion

The area around station 5 has an exceptionally high water table and there is evidence of ground water seepage through the bed. Seepage through the banks above the stream surface indicates that the water table is at least one foot higher than the stream surface during base flow. This ground water intrusion is seen as eruptions in the stream bed. Small areas where sand particles are continually in motion, usually rising a short distance from the bed before settling, are present throughout this area. A schematic of this piping phenomenon is shown in Figure 5. Though visual evidence of this type is only observed in certain locations, it may not mean that intrusion is restricted to these small fluidized areas. It is possible that seepage is occurring throughout the bed and just at localized areas the bed condition is such that piping occurs.

Normal seepage velocities are of the order of .001 feet per second (Todd, 1959) with values as high as .01 recorded. From observations of the piping condition at station 5, velocities have been estimated in the range of stream velocities, i.e., .1 feet per second. As a result, the flow in the local piping area behaves like a turbulent jet. The

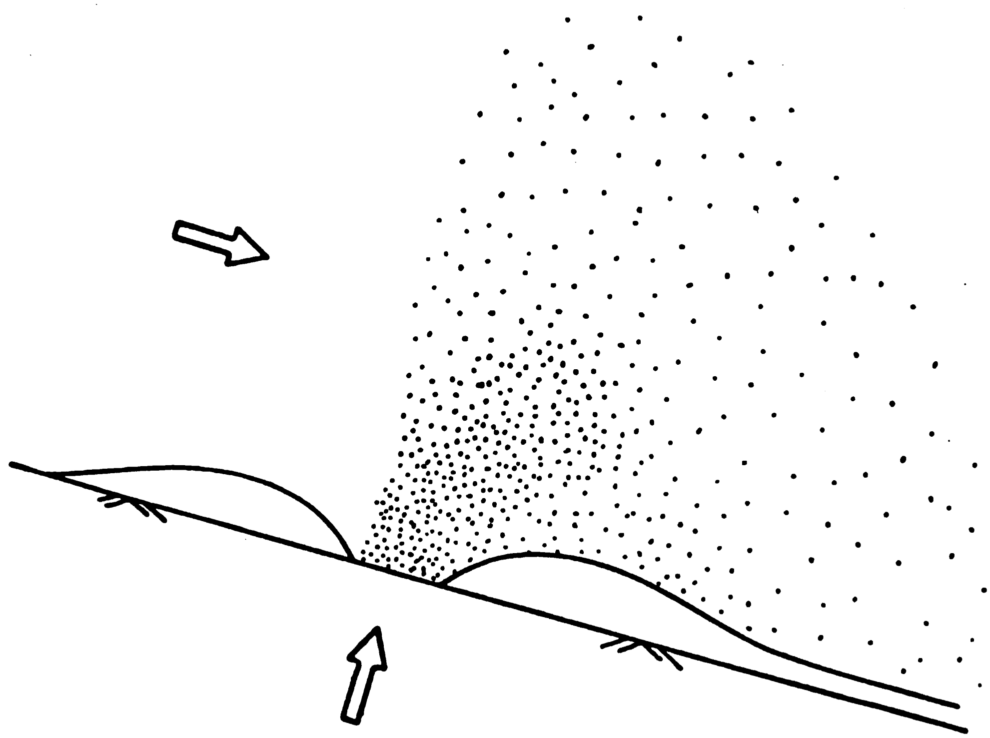

Figure 5. Piping Phenomenon

eruption of particles indicates that the vertical force due to the seepage velocities is dominating all other forces. The horizontal flow of the stream cannot sustain entrainment and the particle settles to the bottom a short distance downstream from the piping area. Particles do not build up downstream because the drag force causes a spreading of the sand grains over the bed. As a result, non-cohesive sand grains are available for entrainment.

The character of the eruption is indicated in Figure 10. Concentration measurements were made at several locations in the vertical and horizontal to establish a grid over the entrainment site. Measurements were made at .5, 1, 2, and 3 inches above the bed and at several points along the bed. The strength of the turbulent jet is indicated by the concentration traces for each elevation.

Solving the incipient motion equation for areas where piping was not occurring yields a value of 20 degrees for the angle of repose (Appendix A). This value was obtained from an analysis without considering the possibility of cohesive forces. The angle of repose was measured by two different methods: one which reduced the cohesive effects and another in which the effects were a factor. The first method allowed the soil particles to free-fall in the fluid and a value for the angle of repose of 23 degrees was measured. The second procedure involved a probe pushed through a mound with the bank allowed to stabilize. This method stresses the importance of the cohesive properties of the sediment and an angle of repose of 41 degrees was determined. This indicates that the non-cohesive angle of repose of the bed can be roughly estimated by use of the incipient motion equation.

The only insignificant force for the conditions at station 5 is

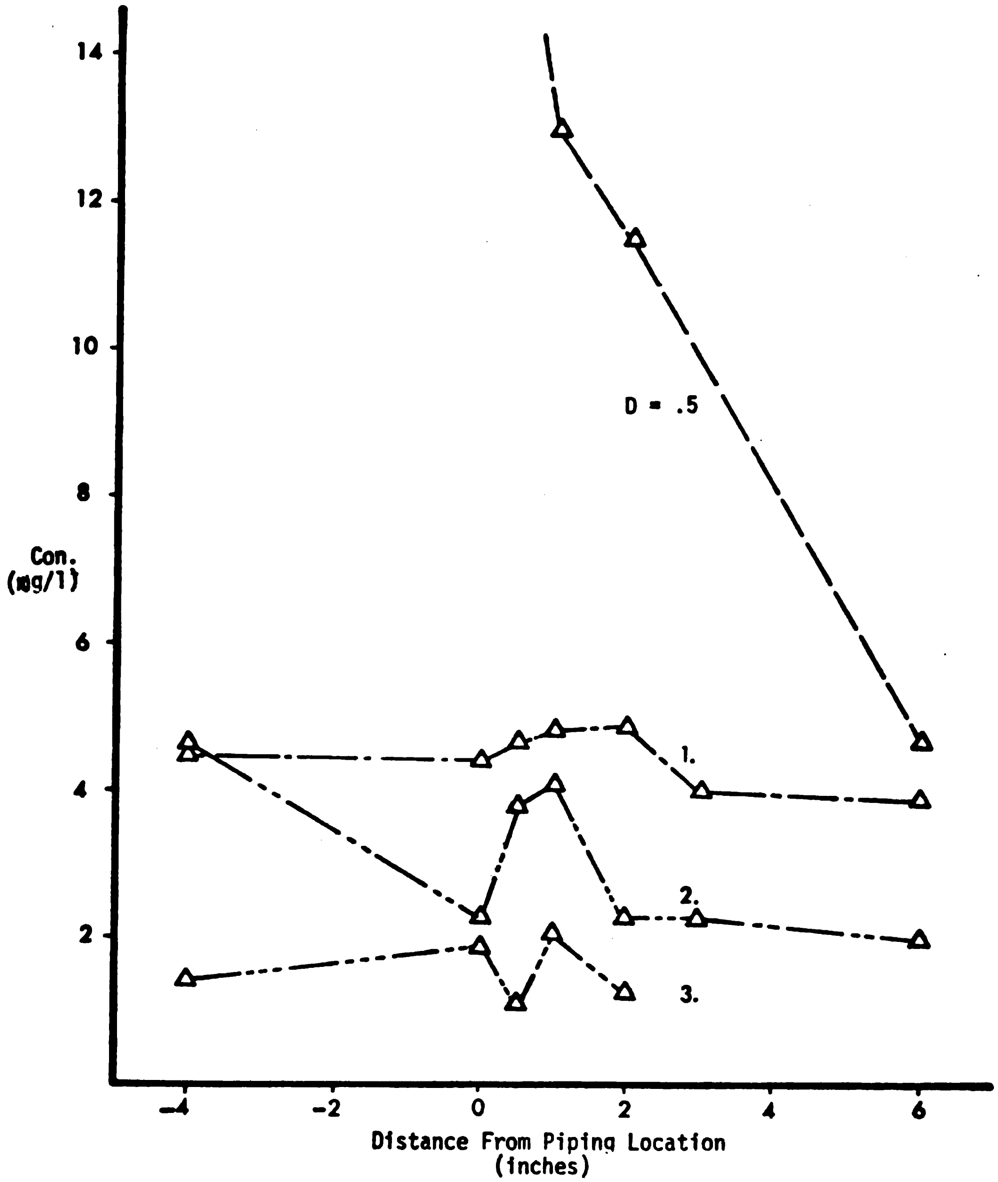

Figure 6. Concentration Traces at a Piping Location

the shear lift. Martin (1971) measured the piezometric head gradient which produced piping, about 2.5. If this incipient motion criterion held in the piping condition, the seepage force would be dominant.

4.4 Pressure Distribution Around a Particle

The resultant forces discussed in the previous section treats each force individually and does not take into consideration the interactive nature of the problem. Seepage causes an alteration of the boundary layer which has a direct impact on the hydrodynamic forces. In addition, it is not totally correct to separate the lift from the bouyant weight in that (1) hydrostatic pressure is not necessarily present under the sphere and (2) the lift accounts for the total pressure difference. Therefore, an approach which deals with the pressure distribution over the sphere will take into account the interactive nature of the problem. From the pressure distribution analysis, a force perpendicular to the flow and one parallel to the flow can be defined.

In natural stream flows the lift and drag are important hydrodynamic forces. Both are dependent on the pressure distribution over the particle surface. Separation of flow gives rise to significant hydrodynamic lift and drag and enhances the possibility of shear lift.

Without seepage, a condition which may result in flow separation around a particle is shown in Figure 3. As a fluid flows over the particle, the stream lines converge and there is an initial acceleration of fluid resulting in a decrease in dynamic pressure from the upstream side to the top of the particle. Deceleration occurs on the downstream side of the particle where pressure increases and an adverse pressure gradient exists. The motion of the fluid in the boundary layer is retarded by the viscous shear of the particle. As the fluid moves from A to B in Figure 3, kinetic energy is lost due to the viscous shear. Additional losses occur as the fluid begins to decelerate on the downstream face of the particle. As a result, the fluid may not have enough kinetic energy left to flow against the adverse (or positive) pressure gradient from B to C. The fluid flow does not proceed along a symetric streamline in the boundary,motion along the boundary ceases and separation occurs from the region adjacent to the bed particle surface. Since the lift and drag forces are dependent on the pressure distribution over the surface of the particle, a change in pressure distribution resulting from a shift in the separation point will cause these forces to change.

If the energy of the boundary layer fluid is increased, fluid will flow a greater distance along the particle surface before separating. When the separation point shifts downstream the size of the separation zone decreases and the surface area of the particle over which the low wake pressure exists is decreased. This results in a reduction in the lift and drag.

Flow separation may be eliminated if the momentum deficiency of the boundary layer, the cause of the separation zone, is counteracted by discharging fluid from within the particle. For the situation of bed particles immersed in a fluid, fluid is not discharged from the particle but from the bed.

Clark (1965) conducted experiments in the hydraulically-rough flow condition which showed that as effluent seepage discharge increases, flow separation decreases with the expected effect on lift, i.e., the average lift force is reduced. On the other hand, Clark found that for influent seepage variation of lift and drag did not correlate with the magnitude of influent seepage. The similarity between the discharge of fluid from within a particle and the discharge from a bed of particles is apparent for effluent seepage because the seepage discharge expands the viscous boundary layer and strengthens the hydraulically-smooth character of the bed. However, influent seepage draws high energy fluid closer to the bed particles, thus reducing the size of the sublayer increases the hydraulically rough situation. As a result, turbulence plays a greater role in changing the pressure distribution over the particles and its subsequent effects on lift and drag.

The viscous effects on the particles, in particular the shear lift, will be reduced due to the reduced separation and flow reversal. The drag force is also expected to be reduced by effluent seepage and has been experimentally confirmed by Watters and Rao (1971). Therefore, the net effect of seepage through the bed and into the stream is a decrease in the entraining forces. This effect will result from effluent seepage until the seepage flow dominates the transverse stream flow - the point at which the bed becomes quick.

4.5 Turbulent Motion

The concept of turbulent motion is rarely considered in the analysis of forces on bottom particles. The complexity of turbulent flow does not permit analytical solution of the pressure distribution and hydrodynamic forces. By considering the physical picture of turbulence and its effects on sediment transport and bed erosion, a better understanding of the actual flow pattern and hydrodynamic force relationships can be developed.

Consider Figure 7 which represents the vertical velocity fluctuation V' in the midst of turbulent flow. The diagram in Figure 7 (a) can be regarded as the result of superposition of the component diagrams in Figure 7 (b), (c), and (d) which represent the components corresponding to the largest, intermediate, and smallest periods of fluctuation, respectively. Each of the components is interpreted as a disturbance produced by eddies of a certain period and size. The horizontal and fluctuating velocity component U' can be analyzed in a similar manner. The turbulence is the end result of the chaotic motion of a large number of various eddies superimposed on the average motion.

The average period of the eddy motion increases when their size increases. Accordingly, the diagrams in Figures 7 (b) and (c) representing longer periods can be regarded as those corresponding to large eddies, while that in Figure 7 (d) to a small eddy. The eddies of a given order develop from the larger eddies as a result of their instability. In turn, these eddies lose their stability and give rise to even smaller eddies promoting the cascade of energy until the viscosity finally dissipates the energy that is transferred to the smaller eddies. The mean velocity gradient continues to feed the larger eddies, but in turn the energy cascade of the turbulent motion continues to smaller and smaller scales causing larger and larger velocity gradients. Once a disturbance is generated, it propagates through the fluid medium.

The concept of eddies is useful in explaining the nature of turbulent fluctuations. It is pertinent to say that the instability of the flow, and hence, turbulence, is dependent on the geometric boundaries as well as the kinematic viscosity. The characteristic fluctuations

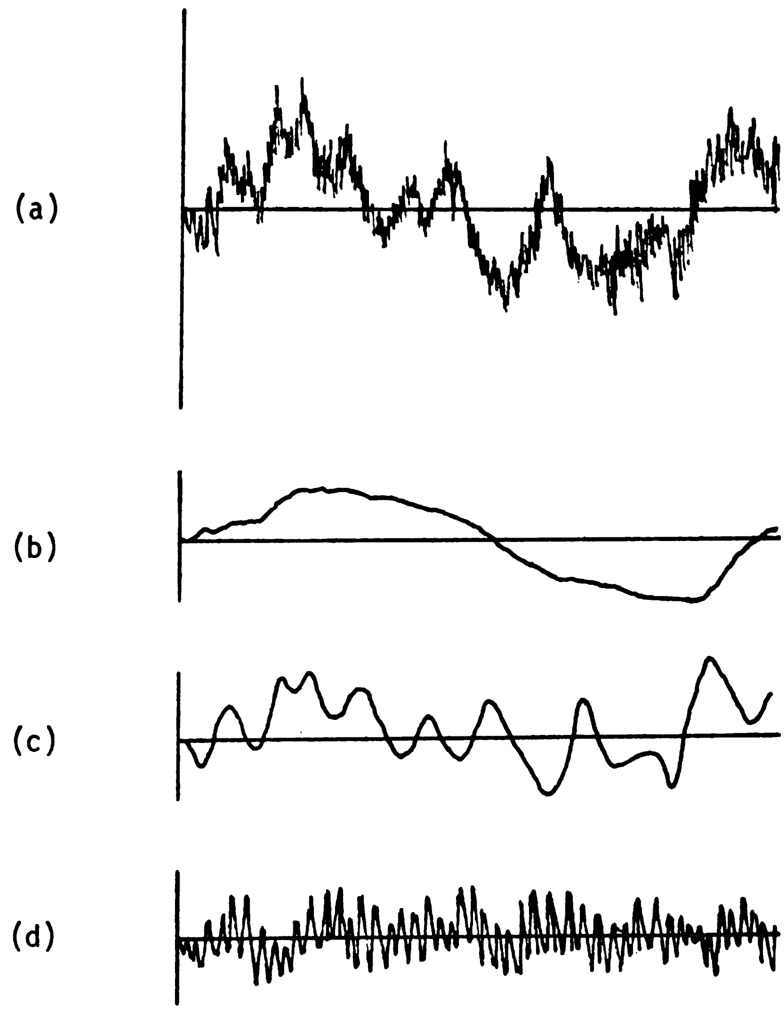

Figure 7. Turbulent Velocity Fluctuations

imposed on a time averaged parameter are due to unstable eddies and the energy cascade.

It should be recognized that in turbulent flow the hydrodynamic forces due to the flow are fluctuating quantities in magnitude, point of application and in direction. Not even the viscous sublayer can be looked upon as steady two-dimensional flow. Studies of the laminar sub-layer have shown a complex flow structure that is dominated by viscosity and large three-dimensional high and low speed velocity streaks. When a high speed eddy from the flow penetrates the sublayer, the boundary ejects low momentum fluid. This low momentum fluid retards the local velocity in the outer region of the boundary layer and can cause another eddy. These high and low velocity regions alternate laterally across the flow and appear as stream-wise streaks on the surface of the flat bed. Thus for natural streams, the bed is subjected to varying bursts of velocity and hydrodynamic force.

Figure 8 shows a time trace of the fluctuating vertical pressure gradient. A certain pressure gradient is required for the lift to dominate the weight force when the particle is entrained. It is possible for the time average mean pressure gradient to be less than that required for entrainment. It is evident from Figure 8 that the instantaneous pressure gradient may cause the particle to lift off the bed while the mean gradient is well below the critical value. Lyle's (1972) flow visualization analysis supports this phenomena in that particles fluctuated at different frequencies before leaving the bed when the time averaged lift force was below that required for entrainment. Oscillation occurred when the particle lift approached critical resulting from varying pressures and velocites caused by turbulent eddies. With sediment

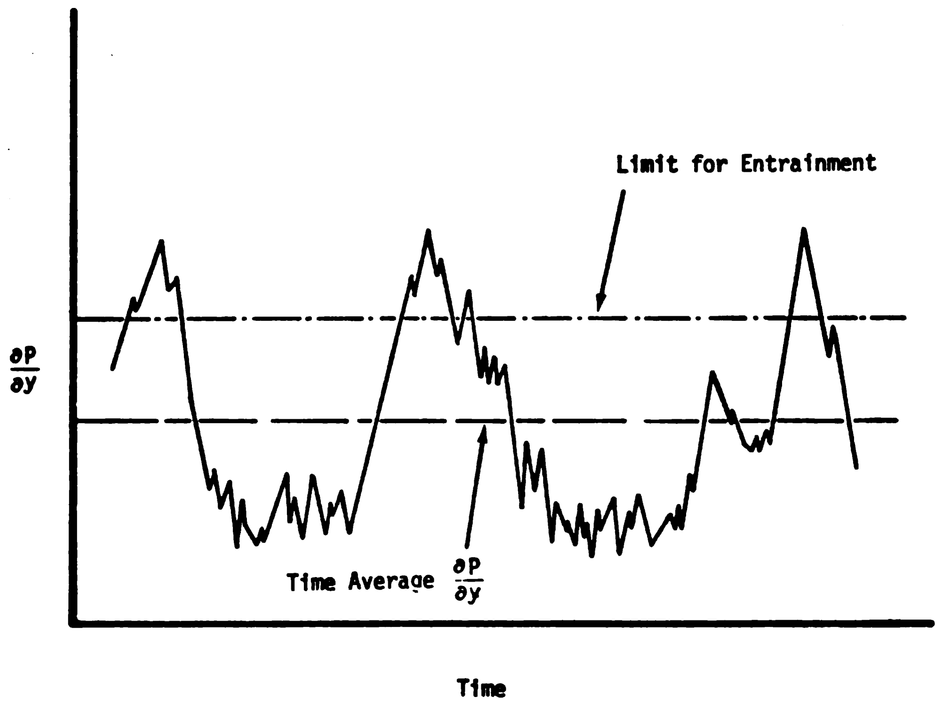

Figure 8. Instantaneous Pressure Gradient

particles available for entrainment, the cascade of energy from eddy to eddy can be passed on to the particle causing entrainment.

The fluctuating pressure gradient gives rise to fluctuating hydrodynamic forces which will at some instant be larger than the time average mean. The importance of turbulence and the instantaneous pressure gradient is apparent.

Turbulence initiates particle motion in several ways. The particle may be moved by the drag exerted by a passing eddy, i.e., an impulse on the particle. It is also possible that particles may be entrained directly into suspension rather than moved along the bed. The vertical pressure gradient may cause a particle to be ejected from the bed due to a decrease in local pressure caused by an eddy.

In natural streams the grains are neither spherical nor of uniform size. As a result, the turbulence level and the hydrodynamic forces are capable in some instances of only moving a portion of the particles. In addition, the problem of defining the maximum instantaneous pressure gradient in a real flow situation makes a stability criterion difficult to develop from the viewpoint of turbulence.

CHAPTER 5

EXPERIMENTAL EQUIPMENT AND PROCEDURES

Data requirements for the study include the basic hydrological network - precipitation and stream flow. In addition, suspended sediment samples as well as pesticide determinations were obtained on both event and seasonal basis. Localized sediment entrainment measurements were required to investigate the effect of ground water intrusion through the stream bed.

The portion of the Mill Creek Watershed (Figure 9) of interest is that northwest of highway M-37, which forms an interior watershed boundary. This portion of the catchment is primarily orchard growing area with appreciable row crop production. As a result, while the majority of the watershed may not be tilled, a considerable portion is cultivated. Consequently, erosion is not uniform in the watershed and variations in sediment and pesticide loadings in the stream can be expected from station to station. In general, the creek may be described as a cold water, usually clean creek with a drainage system representative of midwestern agricultural creek of moderate size and low relief gradient.

5.1 Hydrologic Measurements

Basic hydrologic data available from May, 1975, to the present consists of continuous records of precipitation at three sites and stream stage at two locations. The three Bendix precipitation gages (Model

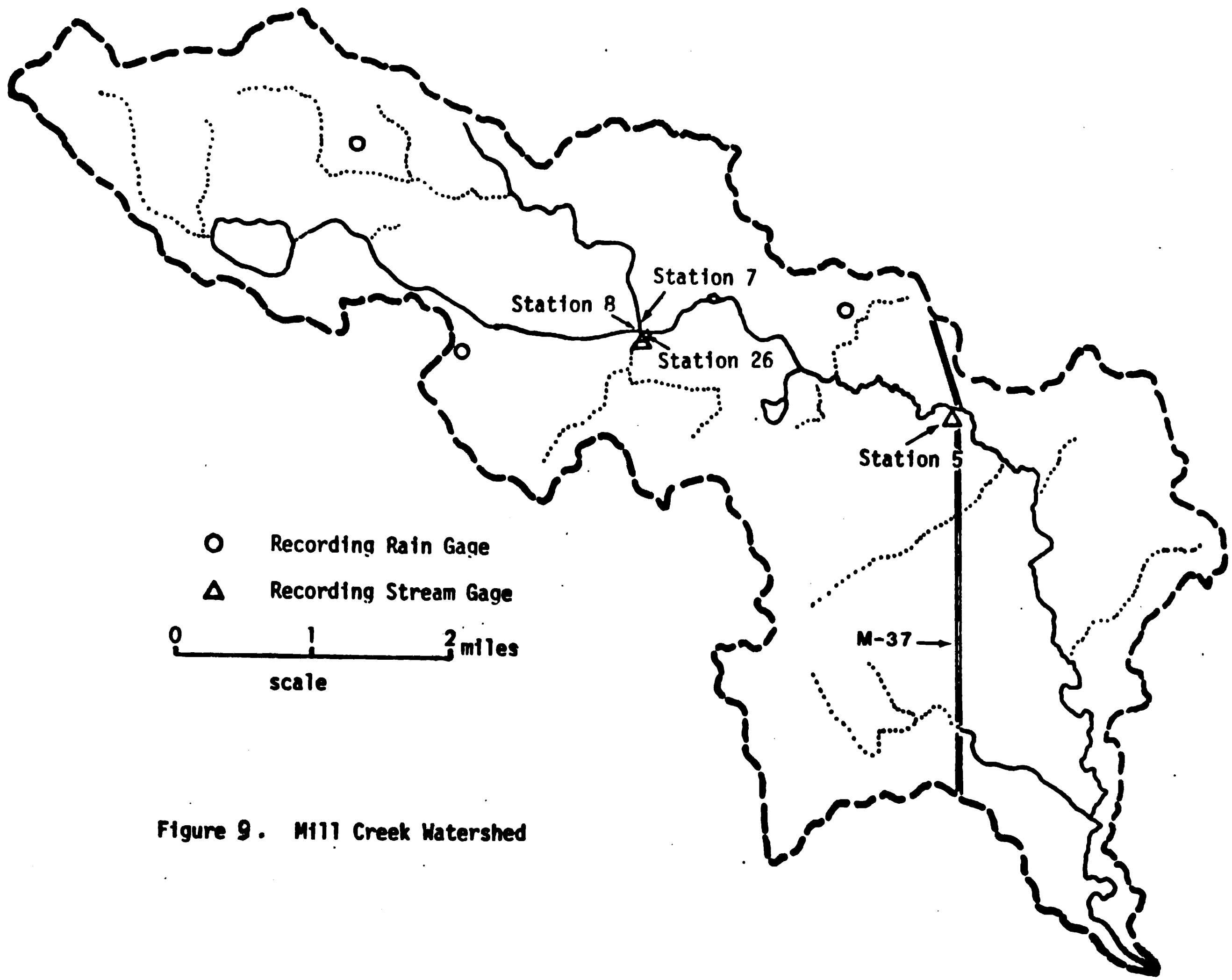

Figure 9. Mill Creek Watershed

775C) are located in such a fashion that a representative average rainfall can be evaluated for the entire watershed. Other manual rain gages were utilized to supplement and check the recording gages.

Stream stage height was continuously recorded at two locations along Mill Creek by means of a Stevens' type A-71 recorder. In conjunction with the continuous recorders, staff gages were placed at the appropriate locations for an index of stage elevation. The location of the precipitation recorders and stream gages are shown in Figure 9.

The stage recorder at station 5 is located at the upstream side of the culvert for M-37 and measures the runoff from the entire northwestern portion of the watershed. In effect, measurements at this station give the yield of the subwatershed of interest. The control for this section is the box culvert at M-37 and because of the flat sandy bottom, it is possible to obtain a reliable conversion for discharge. Station 26 has a continuous stage recorder and is located on Mill Creek at the downstream side of the confluence with North Branch. This station is approximately three miles upstream of station 5. The controlling section for this station shifts for high discharge, but is normally a shallow pool downstream of the confluence east of which the gradient of the creek steepens considerably.

Discharge measurements were made at all stations as well as those with stage recorders. A standard pigmy meter (Lawrence Co., L-110) was used for base flow measurements following the standard procedure of the USGS. For high water measurements, the Price meter was employed. Accuracy for the stream flow measurements is three significant figures, or for base flow measurements two decimal places. By noting the staff gage height at the time of the discharge measurements, a rating curve was developed for the stage recorders. The stability of the rating curve depends on the stability of the controlling section at each station, as already discussed. The discharge can be determined from the rating curve and continuous stage record. The discharge at other stations can be obtained by means of an indexing technique, utilizing correlations of discharge made with a continuous recording station.

5.2 Water Quality Measurements

Water quality measurements were made at station 5, 7, and 8. Station 7 is located on North Branch just upstream of the confluence and station 8 is on Mill Creek just west of the North Branch confluence. Suspended sediment measurements were made at all of these stations as well as station 26 with pesticide determinations at stations 5, 7, and 8.

Suspended sediment was measured using two different devices. An automatic pump sampler (ISCO, Model 1392) yielded suspended sediment as well as pesticide measurements over a hydrograph. A hand held sampler was used during other times, principally base flow conditions.

Figure 10 shows the device used for measuring the suspended sediment by hand. It is fashioned after the standard USGS DH-48 sampler, but is not as streamlined. From laboratory open channel tests, the effect of the blunt end was investigated by observing the flow pattern. The test indicated the possibility that the stream lines are deflected near the nozzle opening due to the blunt stopper. To insure against this hydrodynamic effect, an extended elbowed nozzle was adopted. The original intake should have been adequate for most cases because the fluid particles, with less momentum, are deflected before the sediment particles. Tests between the two nozzles indicated no measureable difference in concentration.

The method of obtaining the sample involved two approaches. The sampler was moved vertically through the depth of the stream at one location to obtain a depth integrated sample. This is the standard USGS method for determining the average concentration at one location in the stream. The other method was to take several samples at different depths and integrate the concentrations over the depth. Both methods yield similar results, but the second method was much more accurate for higher concentration gradients. A comparison is shown in Table 1. Concentration distribution measurements were made for depths up to two feet. The gradient was such that either method yields satisfactory results. All concentrations after mid-summer were results of integrated point-samples. For the shallow depths encountered at station 26, as low as .3 feet, one sample was taken at approximately the mid-depth point. Measurements of the concentration gradient there indicated that this procedure is satisfactory.

The lateral distribution of suspended sediment indicated that the sediment is fairly uniformly distributed. Table 2 shows the lateral distribution of point samples for a high and low flow case. Similar results were obtained for station 26 where the width narrowed from the confluence to approximately 3.5 feet during base flow conditions. Upstream near the confluence, there was considerable lateral distribution due to the mixing of the tributary and measurements were made to allow average concentrations to be obtained.

After obtaining a hand measurement of suspended sediment, the sample was poured into plastic transporting bottles, remaining capped

Table 1. Comparison of Depth Integration Methods at Station 5.

Test Date	Discharge (cfs)	Depth (ft)	USGS Method Avg. Con. (g/l)	Point Sample Method D*	Con. (g/l)	Avg. Con. (g/l)
4-21-76	6.14	1.3		.23	.006	
			.005	.54	.006	.006
				.77	.005	
4-28-76	2.82	1.0		.1	.014	
				.3	.013	
			.013	.5	.015	.012
				.7	.010	
				.9	.008	

* D = Distance above the bottom / total depth of flow.

Table 2. Comparison of Lateral Distribution at Station 5.

Date	Discharge (cfs)	Location-Distance from east bank (ft)	Point Concentration (g/l)
3-5-76	300.	4.	.154
		8.	.151
		12.	.149
7-2-76	4.65	5.	.010
		7.	.010

until analysis. The possibility of sediment coagulation and adhesion to the plastic container wall was checked. Table 3 shows that any effects of the plastic are hidden by inaccuracy due to the filtration process.

Table 3. Comparison of Sample Containers

Test Date	Sample Container	Point Concentration (g/1)
10-7-76	glass	.0023
	plastic	.0026

Automatic pump samplers are located at stations 5, 7, and 8 for measurement of pesticide and suspended sediment on an event basis. The pump is triggered by a small rise in stage height varying from .1 to .3 feet as measured by the stage recorder. Eight samples are pumped, one every 770 seconds, into a one gallon glass bottle. Each sample bottle represents the average over 1.7 hours. Twenty-eight sample bottles are filled over a two day period, the average time for a hydrologic event to pass through the watershed.

Comparison of the results obtained by the hand sediment sampler and the automatic pump sampler indicate that for higher flows, good correlation exists but for low flows, there is some discrepancy. Figure 11 shows the suspended sediment analysis for the high flow situation of May 6, 1976. The automatic pump sampler yields samples averaged over a 1.7 hour interval while the hand sample gives an instantaneous measurement. From the figure, the results of both instruments give

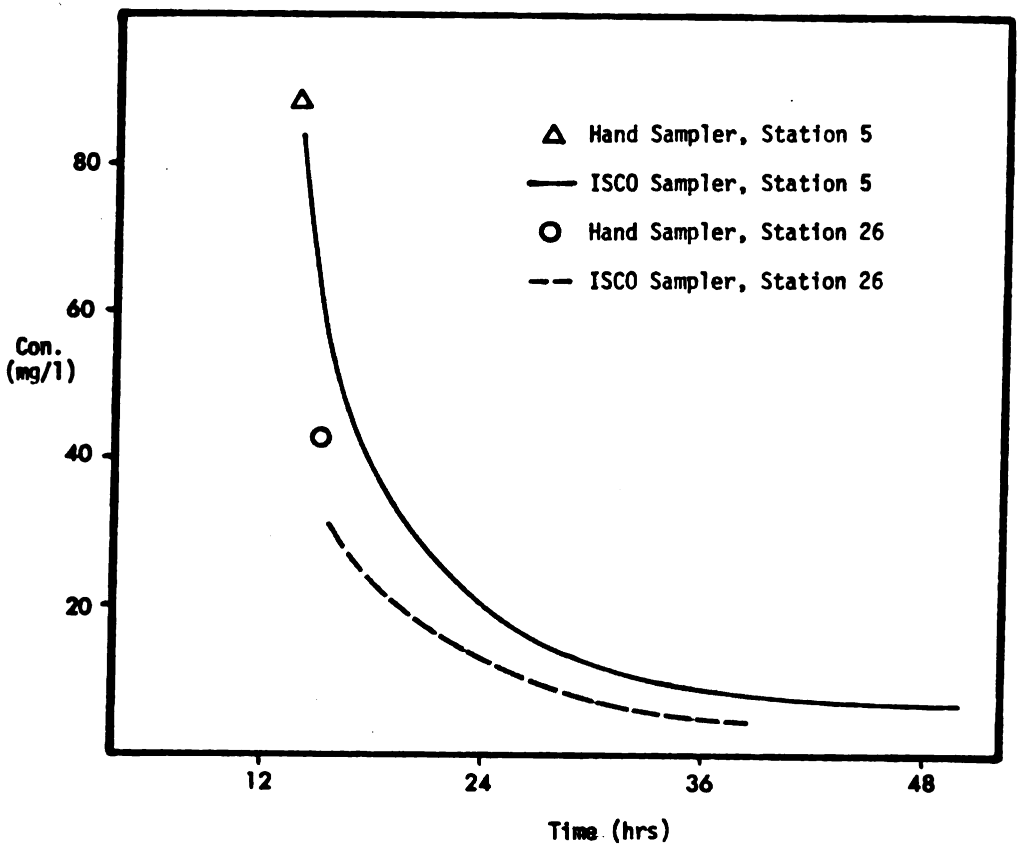

Figure 11. Comparison of Samplers - May 6, 1976

good correlation. For the low flow situation in Figure 12, scatter in the results from the automatic pump sampler creates problems in analysis, but the hand sampler gives results in the same range.

The maintenance of automatic samplers is handled by the Pesticide Research Center at Michigan State University. In addition, they are responsible for the pesticide determinations. A detailed gas chromatography procedure of the pesticide analysis for both dissolved pesticide and pesticide on particulate matter is given in the report Felton Harron Creek, Mill Creek Pilot Watershed Studies, Work Plan, October 1974 (Institute of Water Research, Michigan State University). Eight different pesticides of the chlorinated hydrocarbon group were analyzed with accuracy dependent on the sample size. For the pesticide samples, accuracy of approximately 1 ppt was obtained.

The suspended sediment analysis followed the procedure outlined in Standard Methods (1971) and Sedimentation Engineering (1975). The samples are usually analyzed within a week, but in some instances two weeks elapsed before analysis was carried out. The standard filtration method is followed using glass-fiber filter disks (Cat. No. AP400 4705) and a Millipore filter holder. The filters are prepared by washing with distilled water, drying in an oven at 103° F for 30 minutes, firing in a furnace at 550° F for 15 minutes, and allowing to cool in a desiccator. A Metler balance capable of five digit accuracy was used to weigh the filters just prior to filtration. The filter was placed in a Millipore filter holder, wetted with distilled water, and suction applied. A volumetric pipet was then used to transfer 200 ml of well agitated sample to the Millipore. The filter was then placed in an oven at 103° F for approximately five minutes and then allowed to dry

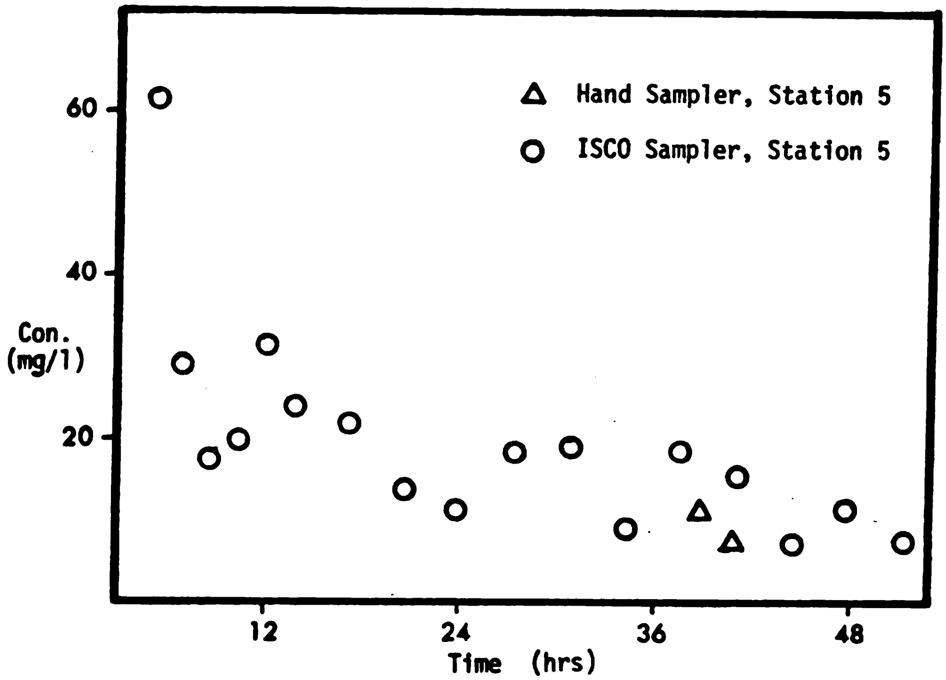

Figure 12. Comparison of Samplers - October 7, 1976

overnight in a desiccator. After reweighing each filter, the weight of suspended sediment for a 200 ml sample could be determined.

To evaluate the accuracy of the analysis, several duplicate filtrations of the samples were conducted. The results indicated that the procedure could be repeated to obtain the same concentration to within 11 percent. The accuracy for base flow concentrations is .0003 g/l, though only with certain samples was the fourth significant figure included.

A Coulter Counter model A was used to obtain a rough indication of particulate sizes in the suspended sediment. One hundred ml of sample was placed in a container and .5 grams of NaCl were added for conductivity purposes. The Coulter probe was then placed in the container and suction applied. Because of the limited volume of sample, only the small orifice probe was used, measuring up to 100 microns. The number of particles were recorded for a given size distribution in terms of volume and then converted to a grain diameter, assuming particles of spherical shape. A blank was required to check for electric field interference and for calibration. Larger particles were examined using a light microscope to determine an average diameter and range.

The angle of repose was measured from bottom samples obtained from the stream bed at station 5. A transparent container filled with water at approximately 55° F was used in the determination of the angle of repose. The sample was fed through a funnel at the water surface and allowed to free fall in the fluid. The slope of the mound which developed at the bottom of the container is the angle of repose (Martin, 1971). Because dispersion of soil particles was evident during settling, another procedure was also used. This procedure involved a cylindrical probe which was passed through a mound at the bottom of the transparent container. As it passed through the mound, the banks behind the probe collapsed. The slope of the collapsed bank gives a good indivation of the angle of repose. Several measurements using both methods were made on different samples to obtain a representative angle.

CHAPTER 6

SEDIMENT AND PESTICIDE TRANSPORT RESULTS

The relevance of stream bed hydraulics and the effects of hydrodynamic roughness on the transport phenomena in the Mill Creek Watershed is evaluated with respect to the translocation of sediment and pesticides during unsteady flow conditions. In order to accomplish this, the sediment transport rate was required, along with the determination of adsorbed and dissolved pesticide levels in the flow. The majority of sediment and pesticide transport occurs during high flows. Therefore, monitoring the stream during periods of surface runoff allows an estimation of the pesticide yield of the watershed. The suspended sediment yield can be calculated by using the suspended sediment transport curve in conjunction with measured stream flow for the entire period of interest.

The effect of ground water intrusion through the stream bed is also of interest. By analyzing the forces on bottom particles under the influence of seepage, the significance of the seepage on particle entrainment can be established.

6.1 Sediment and Pesticide Yield

The analysis of the concentration gradients and particle distribution yields some characteristics concerning the transport of suspended sediment. The suspended sediment samples can be analyzed from these particle transport characteristics and a relationship developed to facilicate calculations of sediment yield.

6.1.1 Suspended Sediment Concentration Profiles

Two methods were used in determining the average concentration in a cross-section. Comparable results were obtained with both methods, (Table 1) but the point sample method utilizes a vertical concentration profile for the stream. The concentration profile is the result of the suspension of sediment due to the hydrodynamic forces. The forces which induce entrainment continue to affect the motion of particles in suspension. If the time average position and force on a particle is considered, then the restrictions on vertical particle movement are the lift forces, both the hydrodynamic and shear, and the particle weight. Because of these restrictions, each size particle should find its equilibrium position in which the lift is equal to the weight. The particle distribution of the sediments available for transport plays an important part in the concentration profile. The lift force is directly proportional to the particle size, as is the weight, so that the density of the sediment dictates the location of the particle. It is entirely possible to find large particles suspended at a considerable distance from the bottom of the channel. An irregular concentration gradient may not be the result of faulty sampling or turbulent fluctuations, but rather an indication of the type of particle distribution. This result has been confirmed for particle concentration profiles in pipes (Zandi, 1970).

Some examples of the vertical concentration profiles as well as velocity profiles for station 5 are presented in Figures 13, 14, and 15 for low and base flow situations. The concentrations do not have a smooth gradient and the possibility of the transport of particles in terms of sizes and depth may be present. The concentration profiles are not of a consistent form, but they do indicate a non-uniform

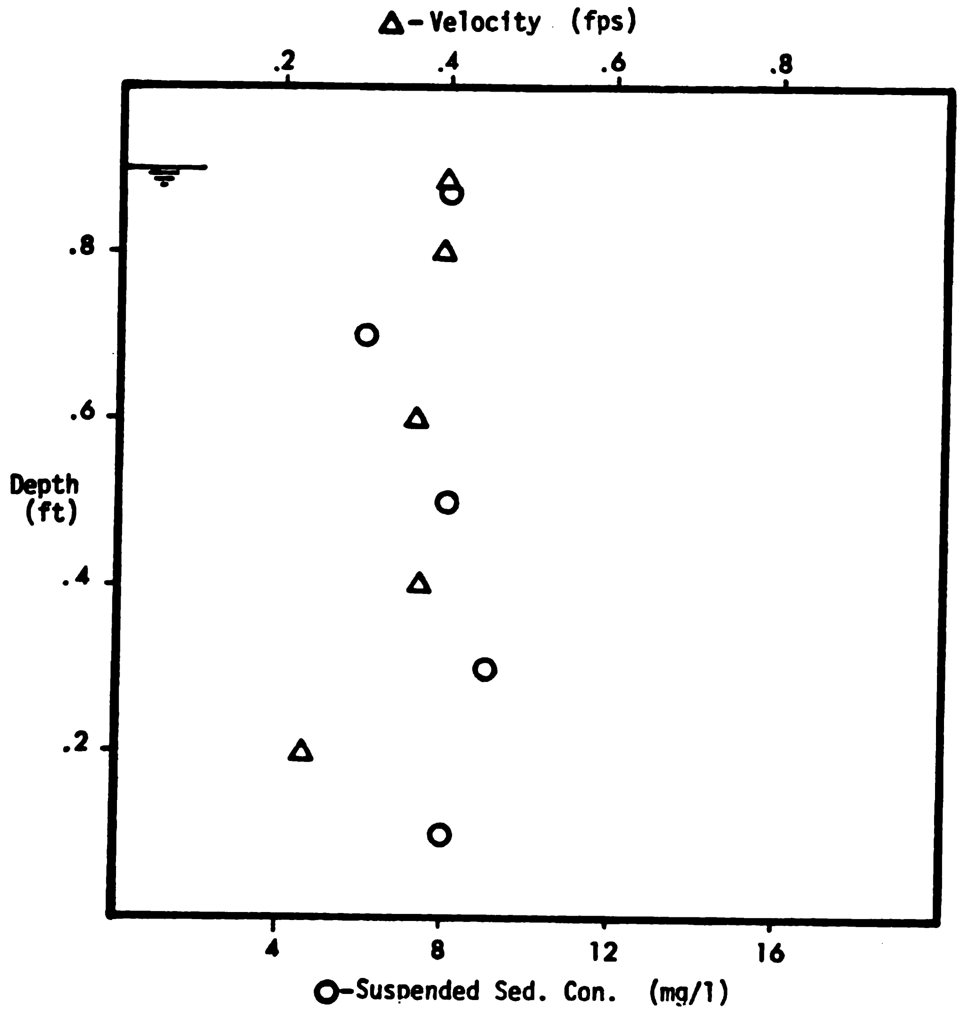

Figure 13. Velocity and Concentration Profile - July 23, 1976

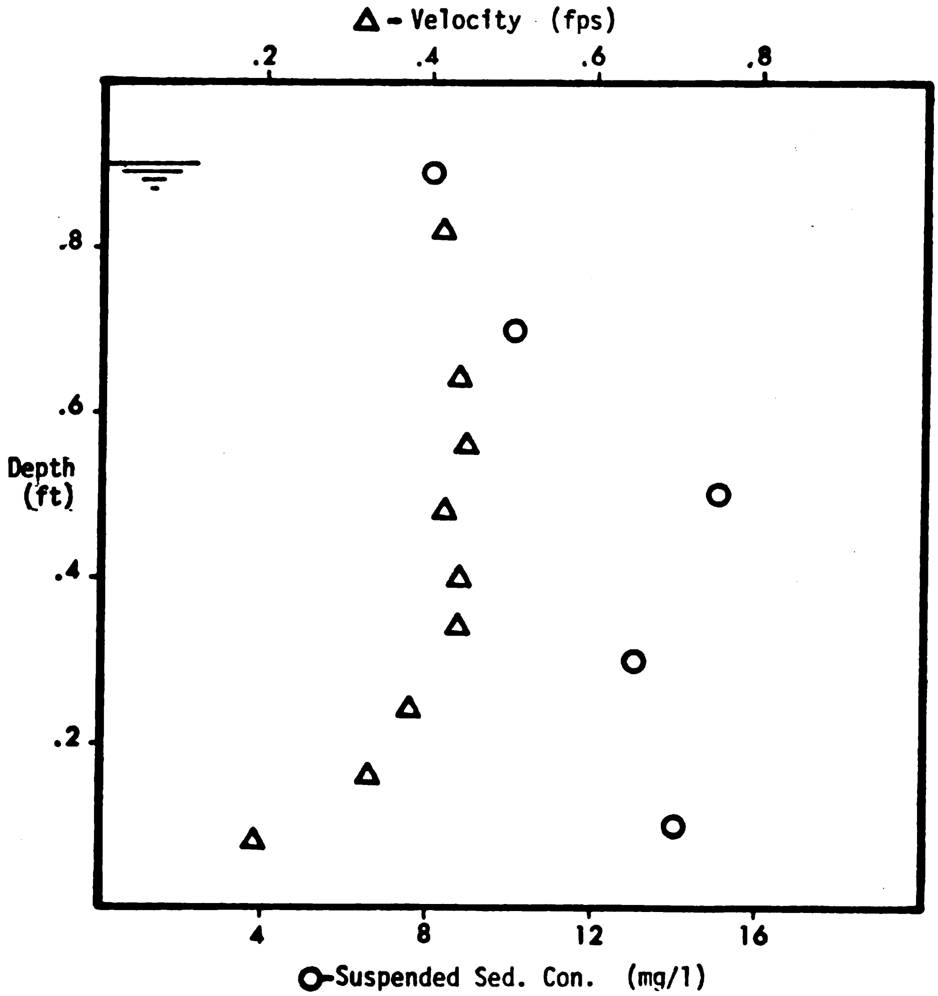

Figure 14. Velocity and Concentration Profile - July 28, 1976

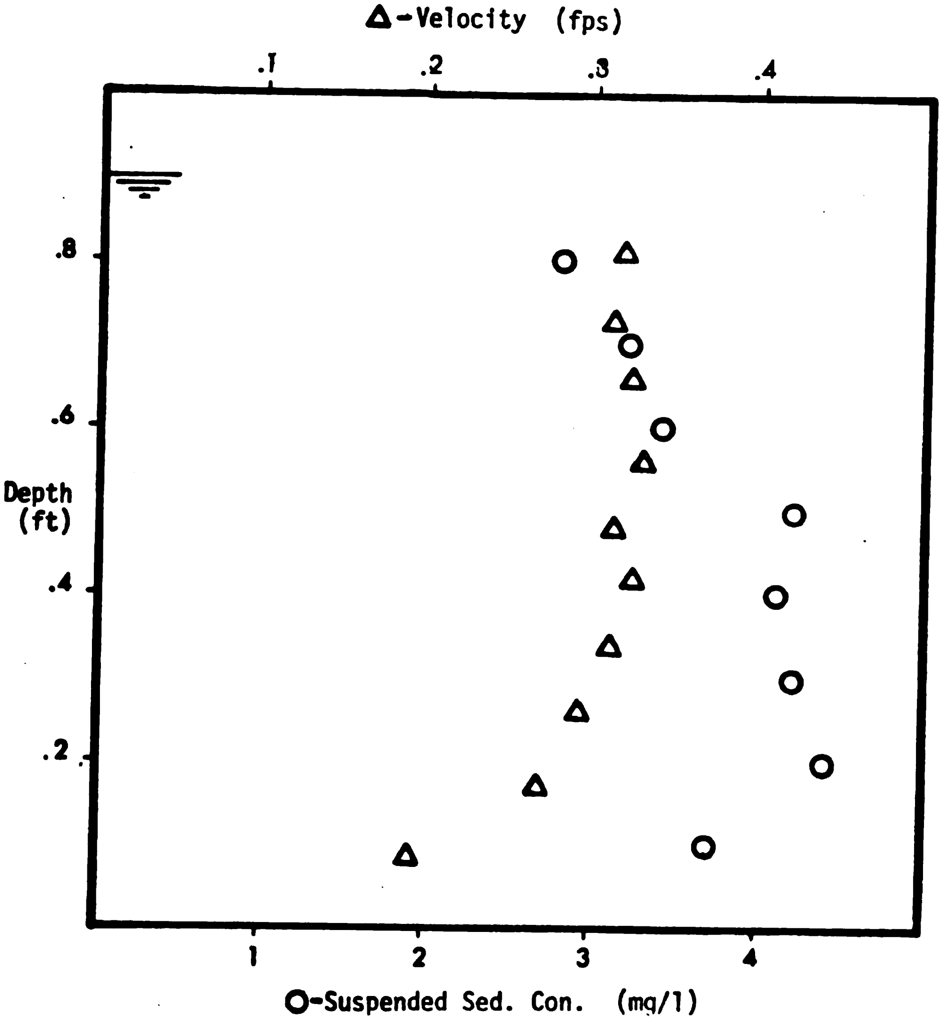

Figure 15. Velocity and Concentration Profile - August 30, 1976

profile exists. Therefore, sampling procedures should include contributions from several depths.

6.1.2 Suspended Sediment Particle Sizes

From the Coulter Counter analysis, a particle size distribution was developed. Figures 16, 17, and 18 show the representative size distribution for samples taken in the fall of 1976. The figures are included to give an indication of the particle sizes present and not to give an exact distribution. The results of the analysis indicate that the mean particle size is between 30 and 40 microns and classified as fine sand and silt. The Coulter Counter analysis had a particle size range up to 100 microns and for larger sand grains a light microscope was utilized.

From the light microscope analysis, the mean sand grain was determined to be 140 microns with sizes up to half a millimeter in diameter. This analysis was for a sample in which 130 particles were measured with a standard deviation of 70.

A different size distribution will occur during periods of runoff due to the introduction of small particles with the wash load and entrainment which occurs with high flows. For low and base flow conditions, the average particle size is 35 microns.

6.1.3 Suspended Sediment Transport Curve

The suspended sediment discharge is the product of the concentration of the suspended sediment sample and the stream discharge at which the sample is taken. By taking several samples at different flow rates during the period of investigation, it is possible to develop the suspended sediment transport curve. Figure 19 shows the relationship developed for station 5, the mouth of the agricultural watershed. A least

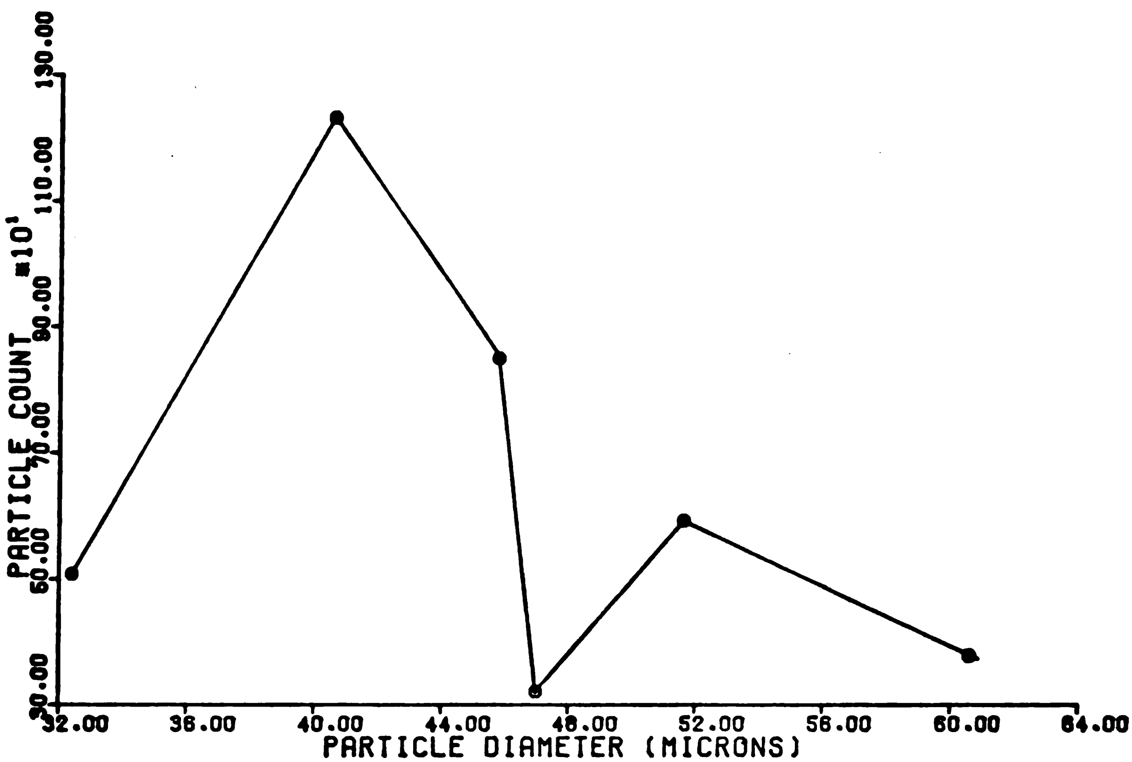

Figure 16. Particle Sizes - October 7, 1976

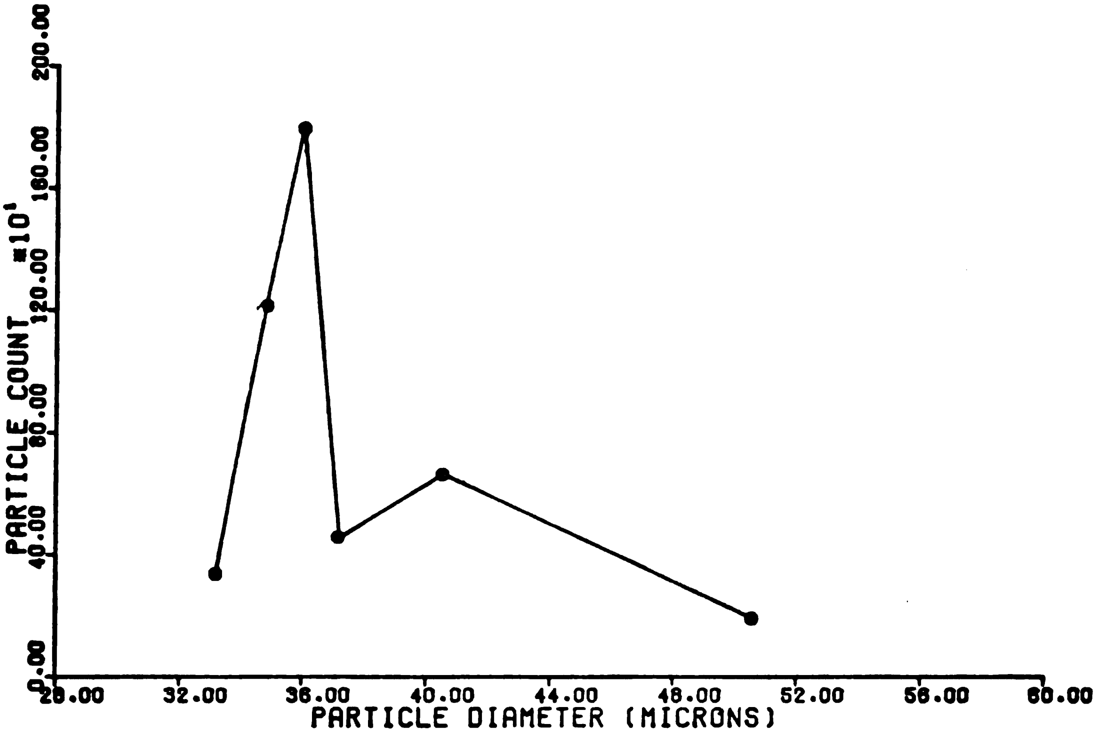

Figure 17. Particle Sizes - October 28, 1976

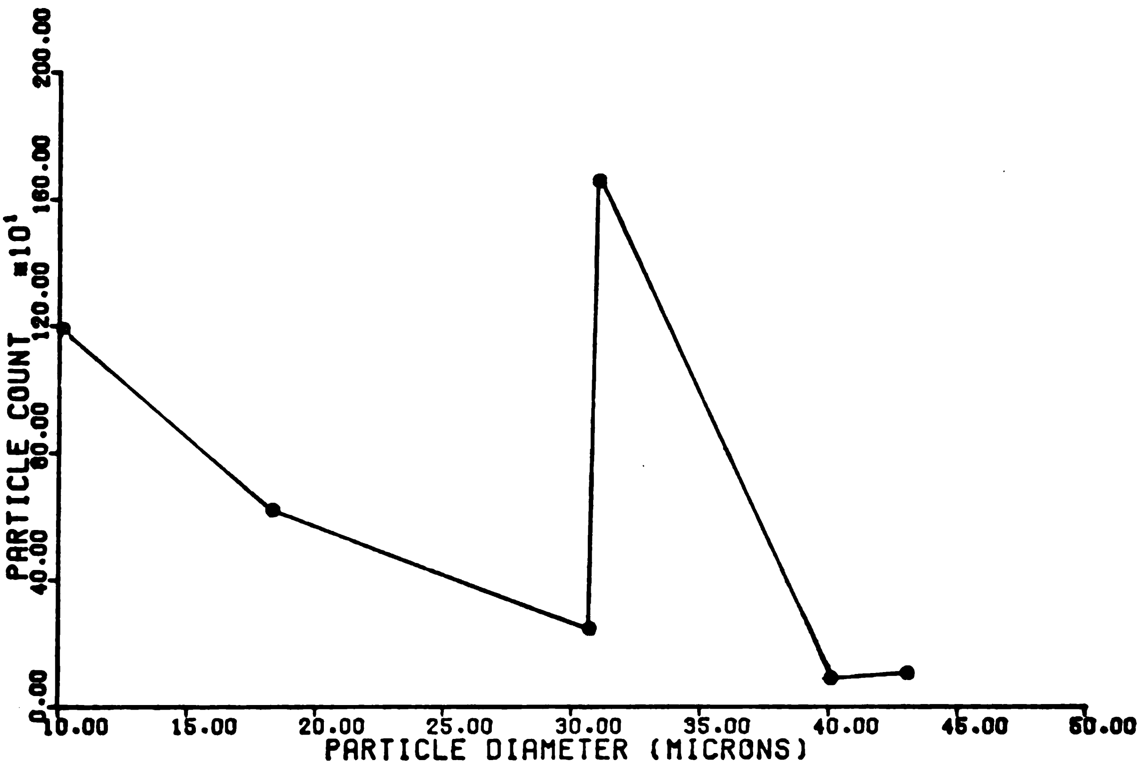

Figure 18. Particle Sizes - November 11, 1976

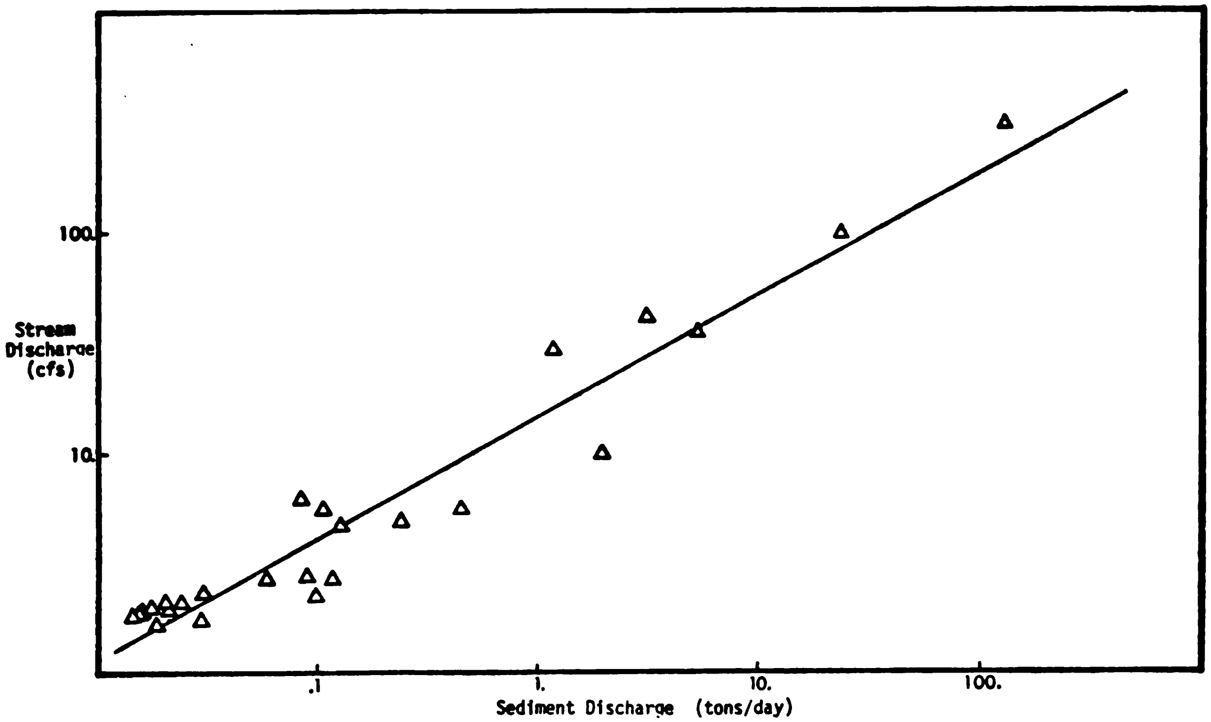

Figure 19. Suspended Sediment Transport Curve

squares fit to these data resulted in the following equation:

$$Q_s = .0078\ Q^{1.81} \tag{13}$$

where Q_s is the suspended sediment discharge and Q is the stream discharge. Because orchard watersheds have a smaller percentage of tilled acreage, sediment available for transport is reduced and the coefficient in the sediment transport curve is smaller than the coefficient for a row-cropped mid-western watershed which has a magnitude of .05 (Sedimentation Engineering, 1975). In addition, the Mill Creek channel has considerable foliage along the stream banks. The exponent in the equation describes the rate at which suspended sediment discharge increases with discharge. For large, western watersheds, the exponent can be as high as three. Tests plots in the mid-west have a relationship in which the exponent is between one and two (Sedimentation Engineering, 1975). For a small to medium-size mid-western watershed, an exponent of 1.81 is reasonable.

6.1.4 Sediment Yield

The sediment yield or total sediment loss during a year is computed with the aid of the suspended sediment transport curve as well as measurements made during unsteady flow. In addition to the suspended load, the bed load must be estimated to obtain the total sediment yield.

The method used to estimate the bed load was developed by Colby (1957) and is utilized by the Bureau of Reclamation. The procedure requires the mean stream velocity, stream width, mean depth, the measured mean suspended sediment concentration and the concentration of the bed sediment. The first four parameters are obtained directly from stream discharge and suspended sediment measurements. The concentration of the bed sediment is determined by extending the suspended sediment profile to the bed and estimating the concentration.

The sediment yield due to the suspended load can be calculated by multiplying the measured mean suspended sediment concentration by the stream discharge. Otherwise, the suspended sediment transport curve is used in conjunction with the continuous stream discharge record. With the mean daily stream discharge known, the suspended sediment discharge can be determined which gives the sediment yield for a particular day. This technique allows the suspended sediment yield to be estimated when no sediment record is available. Combining the use of measurements and the suspended sediment transport curve allows the suspended sediment yield to be determined.

The suspended sediment yield for the hydrologic year 1975-1976 is 730 tons and the bed sediment yield is 65 tons. The total sediment yield for that period is approximately 800 tons. That hydrologic year was an exceptionally dry period in which no significant precipitation occurred after May. Twenty-three inches of precipitation occurred during the year as compared to a normal 30 inches per year. Because of the dependence of erosion on rainfall and the lack of rainfall during the last four months, the sediment loss is less than normal.

Annual sediment yield for watersheds in the mid-west vary from 70 to 900 tons per square mile (Sedimentation Engineering, 1975). Mill Creek's annual sediment yield is approximately 75 tons per square mile, a reasonable figure considering the large percentage of orchard farming and conditions of the stream banks. The suspended sediment discharge agrees well with other small Michigan streams.

6.1.5 Pesticide Yield

Annual pesticide yield for the watershed is not attempted because of incomplete and inconsistent data. The pesticide levels are examined for certain high flows. Data from 1975 indicated that p,p'DDT, Aldrin, and Dieldrin levels adsorbed on sediment were in the part per billion range and dissolved levels in the part per trillion range. A study of Michigan and Illinois waters recorded similar magnitudes for the adsorbed and dissolved pesticides (Schacht, 1974). During the summer of 1976, values of adsorbed and dissolved pesticides for the chlorinated hydrocarbon group were in the low part per trillion range. While this level is consistent for dissolved concentration, the Michigan and Illinois study found much higher levels of pesticides adsorbed on sediments.

The pesticide yields for the events monitored are presented in Tables 4 through 9. The pesticide yield is calculated from concentration measured during runoff. The yield due to dissolved pesticide is added to the yield due to that adsorbed on sediment (the filtered pesticide) to obtain the total pesticide yield for the event. The surface runoff, suspended sediment yield and unit area loading (the total pesticide load divided by the watershed area) are included in the tables. As already established, there is a high degree of correlation between discharge and suspended sediment yield. The pesticide data must be separated by years if any interpretation is to be attempted. The pesticides p,p'DDT, Dieldrin and Aldrin were measured for the summer event of 1975, and the yield is considerably higher than the yields determined for 1976. Possible explanation for this could be that these pesticides have been washed out of the watershed since they are no longer in use. However, before a conclusive statement can be made with regard to this variance in data, a longer period of study is required.

Table 4. p,p'DDT Yield for Several Events.

Date	Surface Runoff (sfd)	Suspended Sed.Yield (tons)	Dissolved Pesticide (lb)	Filtered Pesticide (lb)	Total Pesticide (lb)	Unit Area Loading (lb/sq mi)
6-17-75	20.6	2.0*	.0009	2.8	2.8	.26
5- 6-76	108.	3.2	.0021	.0018	.0039	.00036
5-29-76	21.3	1.0	.0014	.0002	.0016	.00015
6-30-76	3.8	.51	.00003	.00011	.00014	.00001

*Estimated from sediment transport curve.

Table 5. DDE Yield for Several Events.

Date	Surface Runoff (sfd)	Suspended Sed.Yield (tons)	Dissolved Pesticide (lb)	Filtered Pesticide (lb)	Total Pesticide (lb)	Unit Area Loading (lb/sq mi)
5- 6-76	108.	3.2	.0002	.0011	.0013	.00012
5-29-76	21.3	1.0	ND*	.0054	.0054	.00050
5-30-76	3.8	.51	ND*	.0001	.0001	.00001

*ND - not detectable

Table 6. Dieldrin Yield for Several Events.

Date	Surface Runoff (sfd)	Suspended Sed.Yield (tons)	Dissolved Pesticide (lb)	Filtered Pesticide (lb)	Total Pesticide (lb)	Unit Area Loading (lb/sq mi)
6-17-75	20.6	2.0*	3.4×10^{-6}	.68	.68	.06
5- 6-76	108.	3.2	.0004	NA	.0004	.0004
5-29-76	21.3	1.0	.0001	ND	.0001	.00001
6-30-76	3.8	.51	ND	ND	ND	ND

*Estimated from sediment transport curve.
ND - not detectable
NA - not available

Table 7. Aldrin Yield for Several Events.

Date	Surface Runoff (sfd)	Suspended Sed.Yield (tons)	Dissolved Pesticide (lb)	Filtered Pesticide (lb)	Total Pesticide (lb)	Unit Area Loading (lb/sq mi)
6-17-75	20.6	2.0*	1.5×10^{-6}	.06	.06	.006
5-6-76	108.	3.2	.0004	ND	.0004	.00004
5-29-76	21.3	1.0	.0003	ND	.0003	.00003
6-30-76	3.8	.51	ND	ND	ND	ND

*Estimated from sediment transport curve.
ND - not detectable

Table 8. Lindane Yield for Several Events.

Date	Surface Runoff (sfd)	Suspended Sed.Yield (tons)	Dissolved Pesticide (lb)	Filtered Pesticide (lb)	Total Pesticide (lb)	Unit Area Loading (lb/sq mi)
5- 6-76	108.	3.2	.0010	ND	.0010	.00009
5-29-76	21.3	1.0	ND	ND	ND	ND
6-30-76	3.8	.51	ND	.0003	.0003	.00003

ND - not detectable

Table 9. H. Epoxide Yield for Several Events.

Date	Surface Runoff (sfd)	Suspended Sed.Yield (tons)	Dissolved Pesticide (lb)	Filtered Pesticide (lb)	Total Pesticide (lb)	Unit Area Loading (lb/sq mi)
5- 6-76	108.	3.2	.0003	ND	.0003	.00003
5-29-76	21.3	1.0	ND	ND	ND	ND
6-30-76	3.8	.51	ND	ND	ND	ND

ND - not detectable

Analysis of the 1976 data is difficult because the results of only three events are available. Table 4 shows the yields for p,p'DDT. The total pesticide yield decreases with decreasing surface runoff. Because p,p'DDT as well as other chlorinated hydrocarbons were almost exclusively used in the past, this correlation with discharge was anticipated. The yields for DDE and Lindane do not follow this trend in that a higher surface runoff did not produce an increased yield. Dieldrin, Aldrin, and H. Epoxide yields appear to be slightly correlated with surface runoff, but much more data is needed before any definitive relationship between a chlorinated hydrocarbon compound and surface runoff is justified.

6.2 Sediment and Pesticide Time Traces

Suspended sediment and pesticide concentration measurements were made during runoff periods to determine the yield of the watershed as well as any relationships between stream discharge, suspended sediment and pesticide. When the stream discharge recorded during an event is plotted along with the concentrations of suspended sediment and pesticide, a time trace results. From such a graph, it is possible to infer the effect of precipitation and runoff on the sediment as well as the adsorbed and dissolved pesticides.

6.2.1 Description of Time Traces

Figures 20, 21, and 22 are time traces for the pesticides p,p'DDT, Dieldrin, and Aldrin corresponding to the June 17, 1975 hydrograph. The suspended sediment concentration was not analyzed for these samples. The correlation of adsorbed and dissolved pesticide concentration with discharge is apparent in each of these cases. The shape of the pesticide

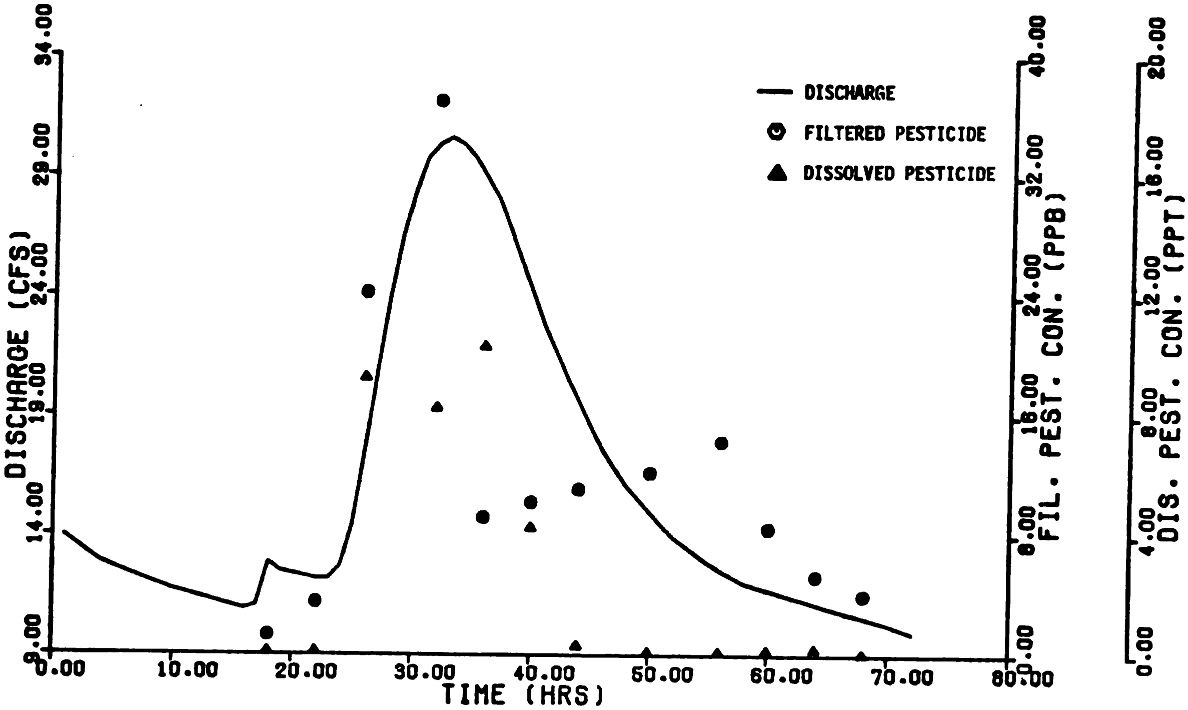

Figure 20.
DISCHARGE-DDT RELATIONSHIP
FOR THE EVENT BEGINNING JUNE 17, 1975

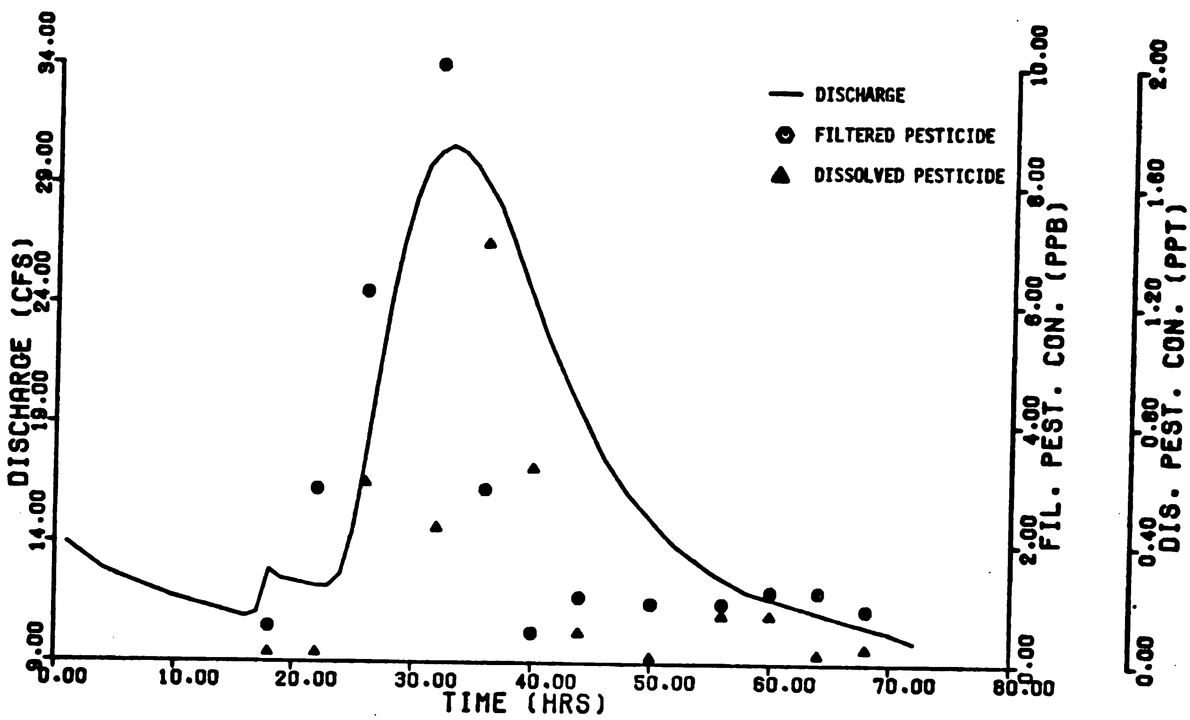

Figure 21.
DISCHARGE-DIELDRIN RELATIONSHIP
FOR THE EVENT BEGINNING JUNE 17, 1975

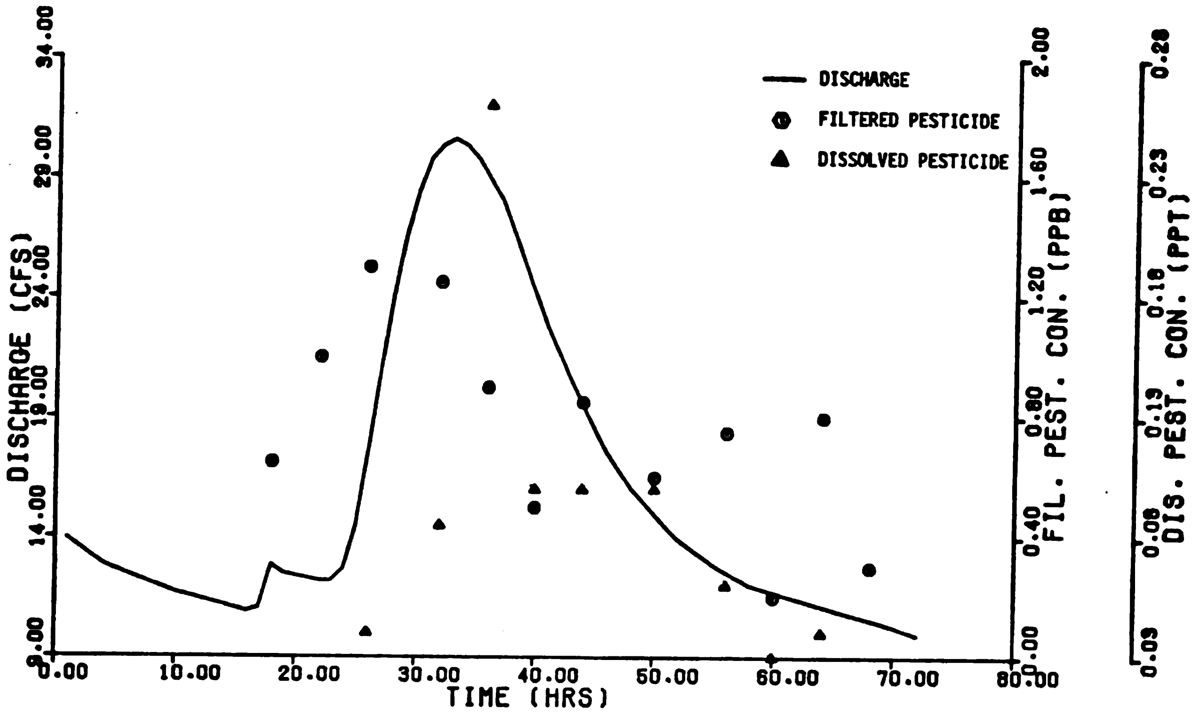

Figure 22.
DISCHARGE-ALDRIN RELATIONSHIP
FOR THE EVENT BEGINNING JUNE 17, 1975

time trace for both dissolved and adsorbed concentrations is similar to the hydrograph for p,p'DDT and Dieldrin. For the dissolved Aldrin concentration, this is true, but the filtered concentration oscillates with the recession of the hydrograph. Figures 23 and 24 show a comparison of the pesticide concentrations for adsorbed and dissolved pesticides, respectively. The adsorbed pesticide concentrations yield similar time traces in that these pesticides are transported by suspended sediment. This is indicated by the quick recession of the pesticide trace after peaking, a common characteristics of sediment. The pesticide p,p'DDT has the highest adsorbed concentration, peaking at about 38 ppb, due to its widespread use and persistence in the environment. Figure 24, the comparison of p,p'DDT, Dieldrin, and Aldrin dissolved pesticide concentration, indicated the dependence of dissolved concentration on stream discharge. The rising limb is steeper than the falling limb, similar to the shape of the hydrograph. The pesticide p,p'DDT has the highest dissolved concentration at about 10 ppb, a reasonable fact in view of its usage.

Figures 25, 26, 27, and 28 show the time traces for the chlorinated hydrocarbon group for the May 6, 1976, hydrograph. The automatic samplers began at about 10 hours, so that most of the rising limb was not sampled. The results show what is anticipated with the recession of the hydrograph. The sediment concentration recedes in a smooth curve to a concentration near that for base flow, .007 g/l. The traces for p,p'DDT and DDE react very similarly, Figures 25 and 26 respectively. There is a slight decrease in dissolved pesticide concentration with a sharper drop in adsorbed pesticide indicating dependence on stream discharge. Figure 27 shows the traces for dissolved Dieldrin and Aldrin.

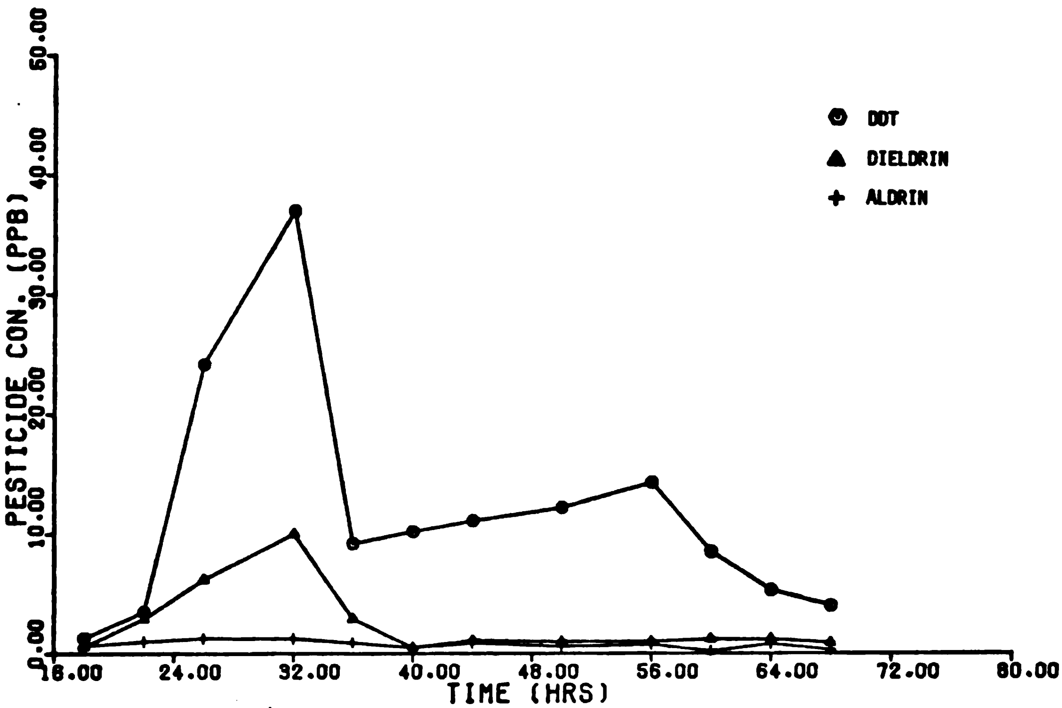

Figure 23.
FILTERED PESTICIDE COMPARISON
FOR THE EVENT BEGINNING JUNE 17, 1975

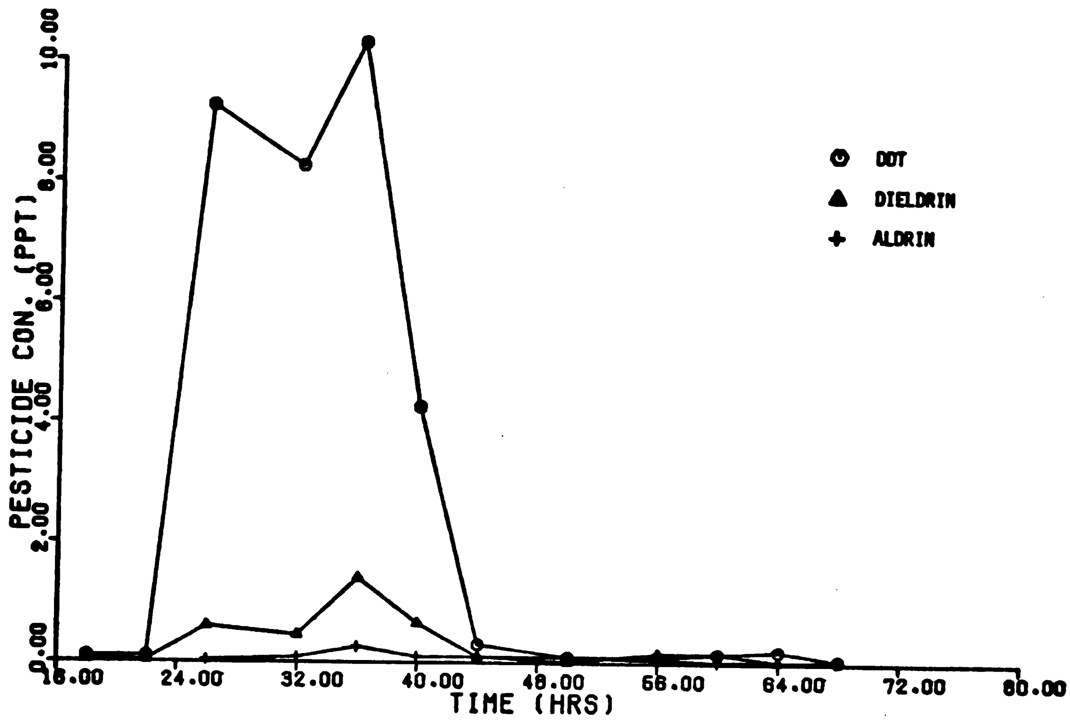

Figure 24.
DISSOLVED PESTICIDE COMPARISON
FOR THE EVENT BEGINNING JUNE 17, 1975

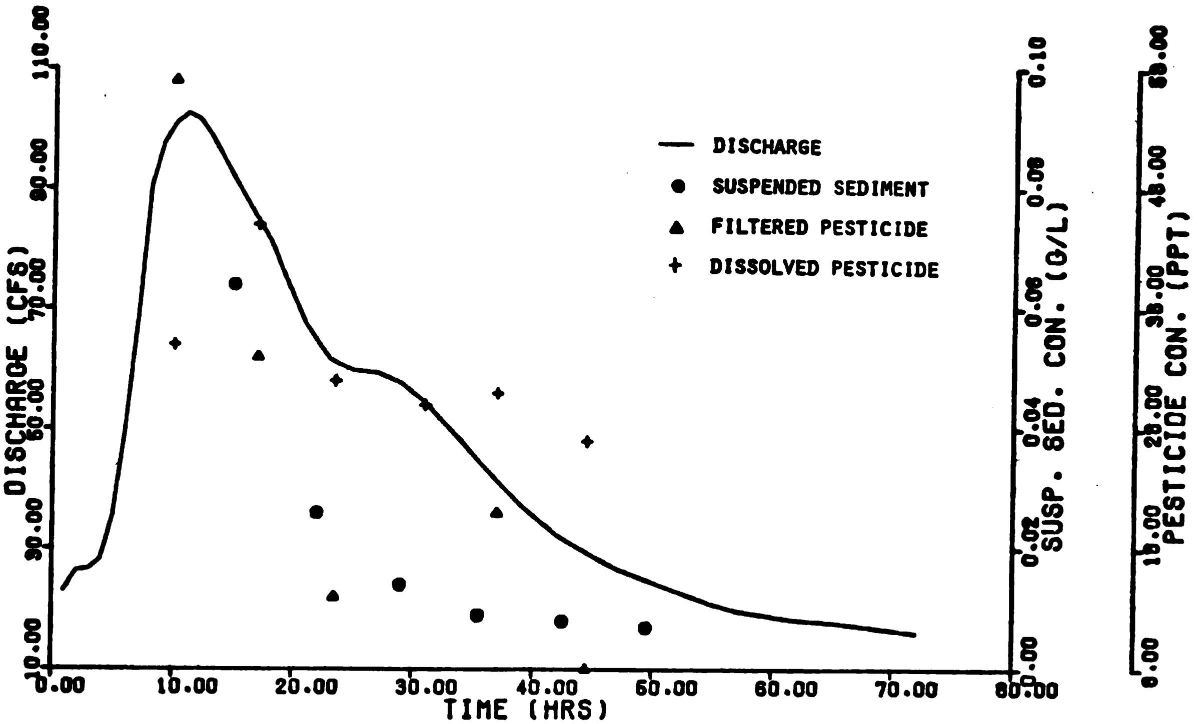

Figure 25.

DISCHARGE-SUSPENDED SEDIMENT-DDT RELATIONSHIP
FOR THE EVENT BEGINNING MAY 6, 1976

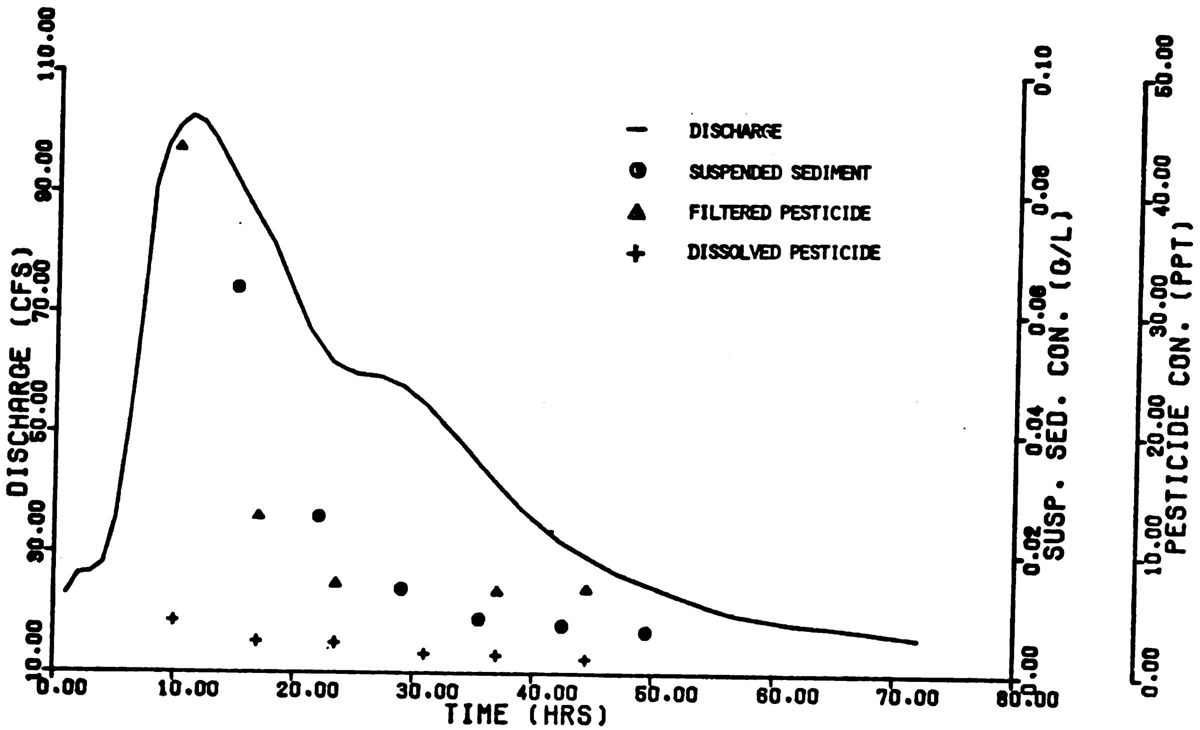

Figure 26.

DISCHARGE-SUSPENDED SEDIMENT-DYE RELATIONSHIP
FOR THE EVENT BEGINNING MAY 6,1976

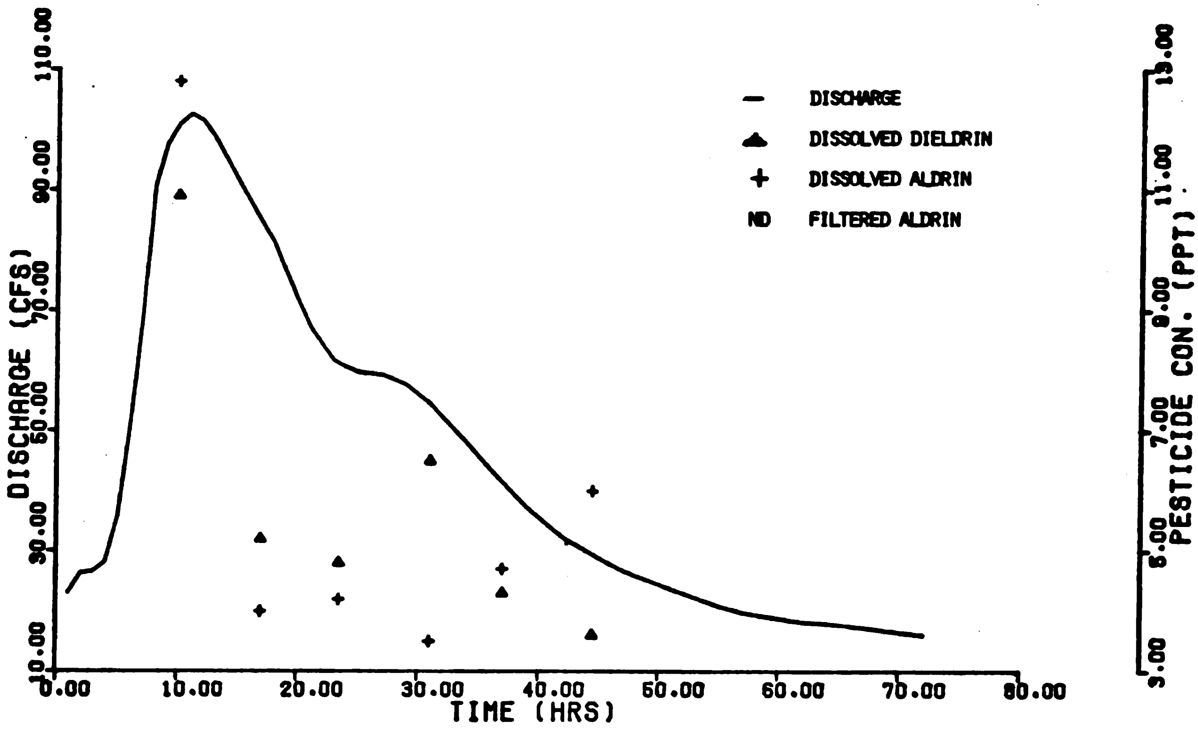

Figure 27.

DISCHARGE-PESTICIDE RELATIONSHIP

FOR THE EVENT BEGINNING MAY 6, 1976

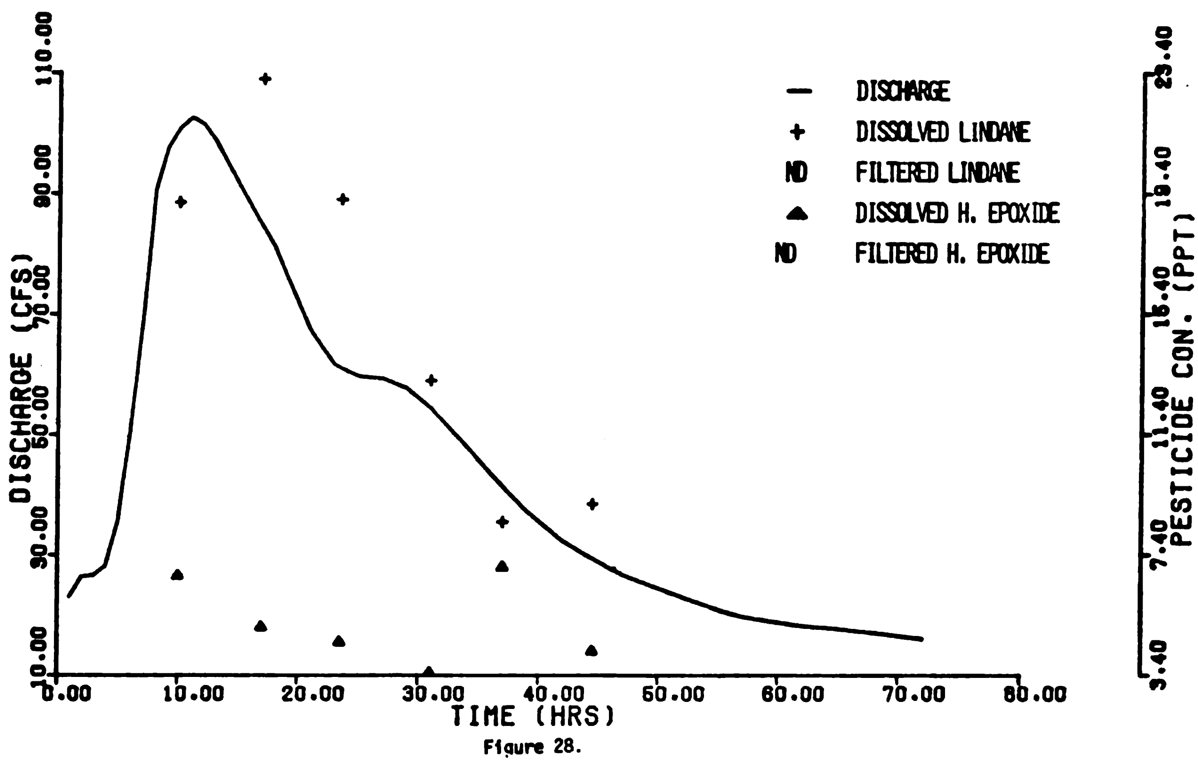

Figure 28.

DISCHARGE-PESTICIDE RELATIONSHIP

FOR THE EVENT BEGINNING MAY 6, 1976

Filtered Dieldrin was not measured and filtered Aldrin was not detectable. There is an overall decrease in concentration along with discharge, although not as well defined as with p,p'DDT and DDE. Figure 28 shows the traces for Lindane and H. Epoxide. A decrease in concentration is again seen with discharge, but like Dieldrin and Aldrin, the correlation is not as good. The better correlation of p,p'DDT and DDE is the result of its widespread usage. Figures 29 and 30 show a comparison of the pesticide time traces for adsorbed and dissolved concentration, respectively. The adsorbed time traces for p,p'DDT and DDE are very similar in shape to that of sediment, a result expected and already explained. The dissolved pesticide comparison shows an increase in concentration with stream discharge, but this is slight for all the chlorinated hydrocarbons.

The hydrograph of May 29, 1975 is shown as Figure 31, 32, and 33 along with the pesticide and sediment traces. This is a considerably smaller event than the two previously discussed and as a result, localized effects are evident. The suspended sediment concentration is low as compared to the other events, taking into account the differing stream discharges. Hydrographs produced by long duration, low intensity precipitation cause this small increase in sediment in the stream. The decrease observed during the hydrograph is the result of less overland flow and sheet erosion. The adsorbed p,p'DDT is relatively stable, but does show some decrease during the hydrograph. The dissolved concentration is highly variable with a general decreasing trend during the event. Filtered DDE shows the anticipated correlation with sediments. Exceptionally high concentration levels were encountered, and it is difficult to explain the origin since DDE is a metabolism of

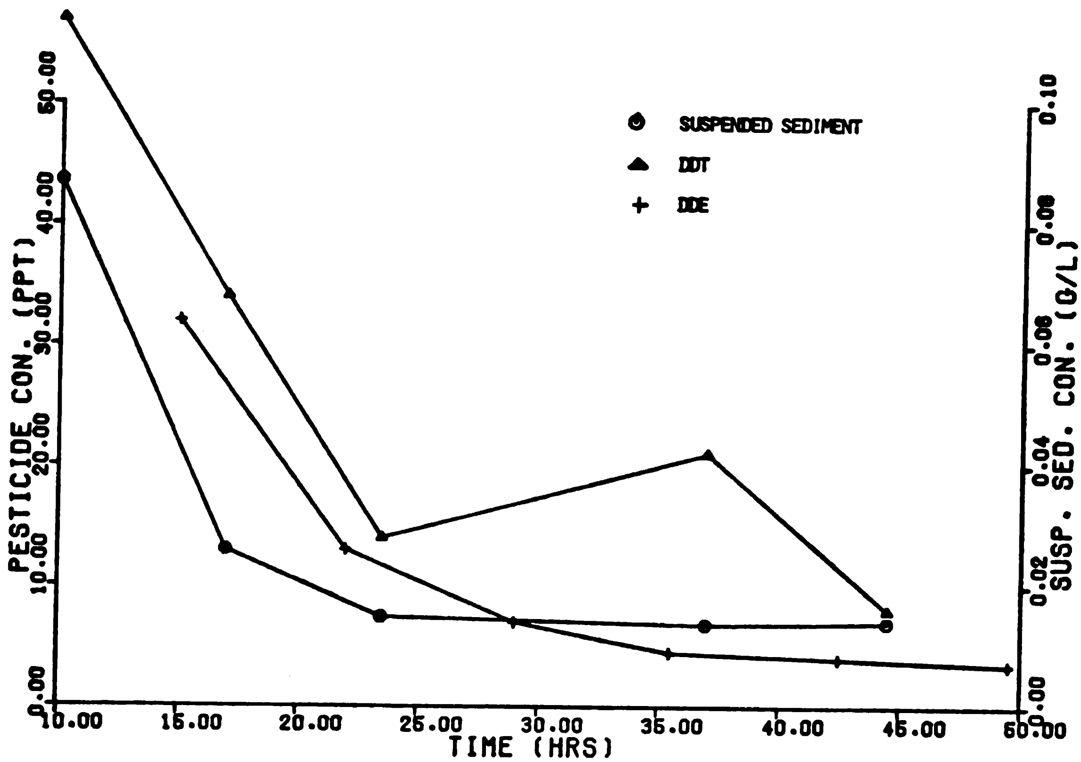

Figure 29. FILTERED PESTICIDE-SUSPENDED SEDIMENT COMPARISON FOR THE EVENT BEGINNING MAY 6, 1976

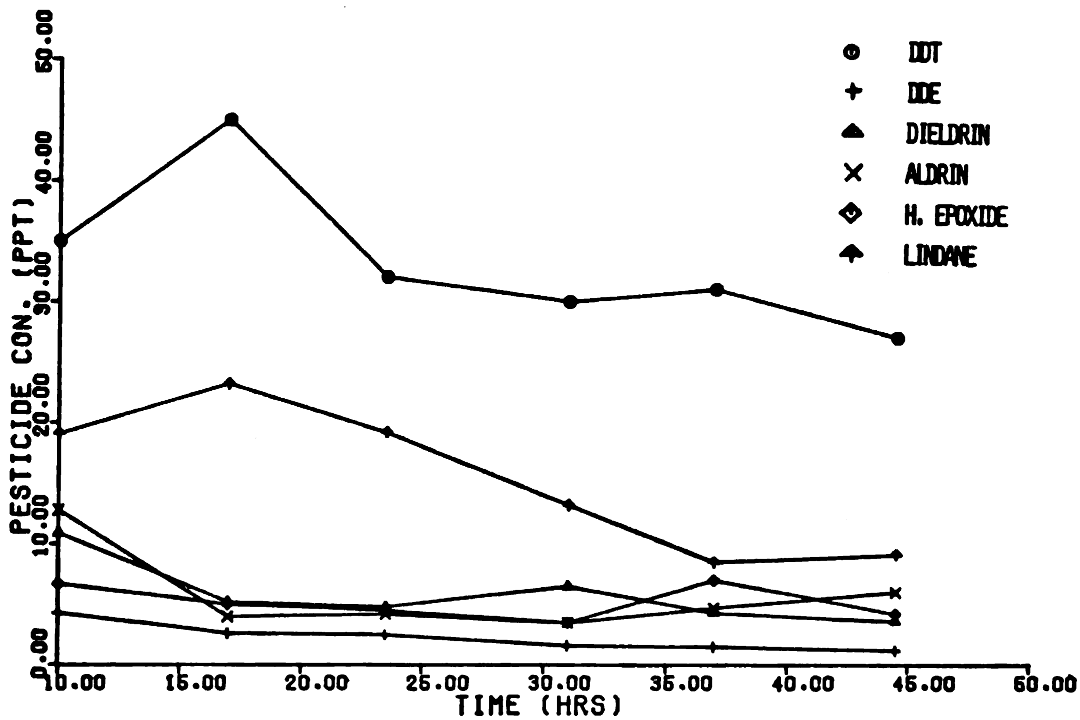

Figure 30.
DISSOLVED PESTICIDE COMPARISON
FOR THE EVENT BEGINNING MAY 6, 1976

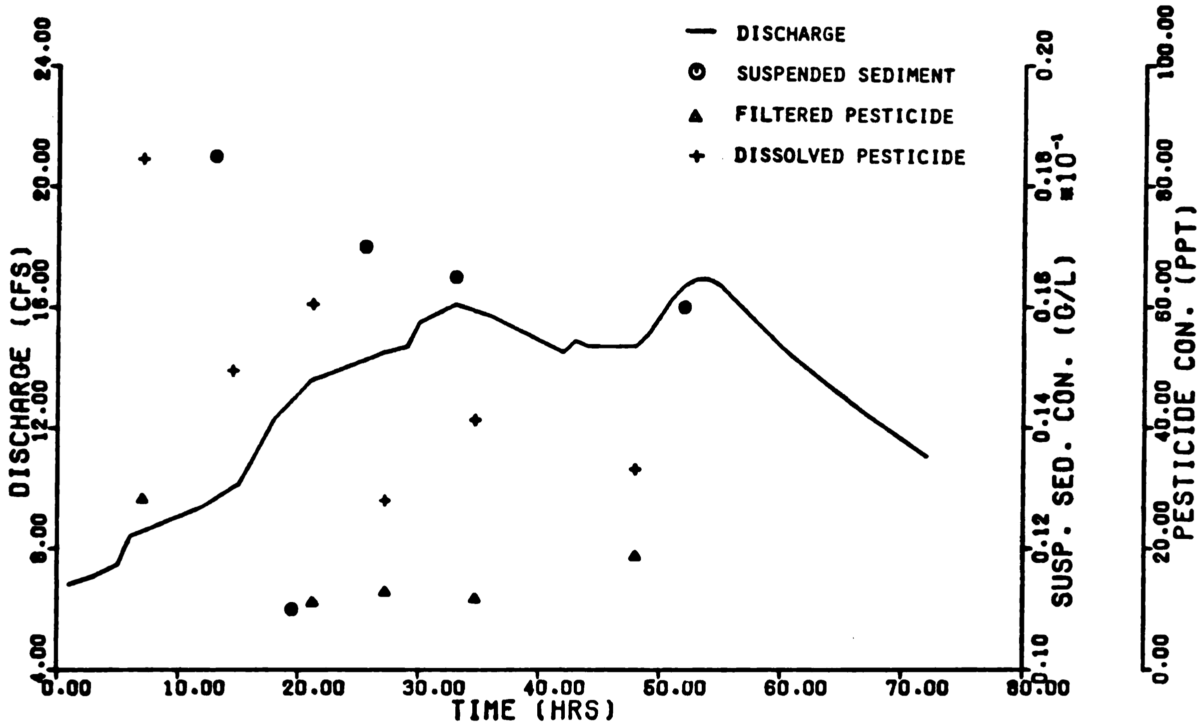

Figure 31.

DISCHARGE-SUSPENDED SEDIMENT-DDT RELATIONSHIP
FOR THE EVENT BEGINNING MAY 29, 1976

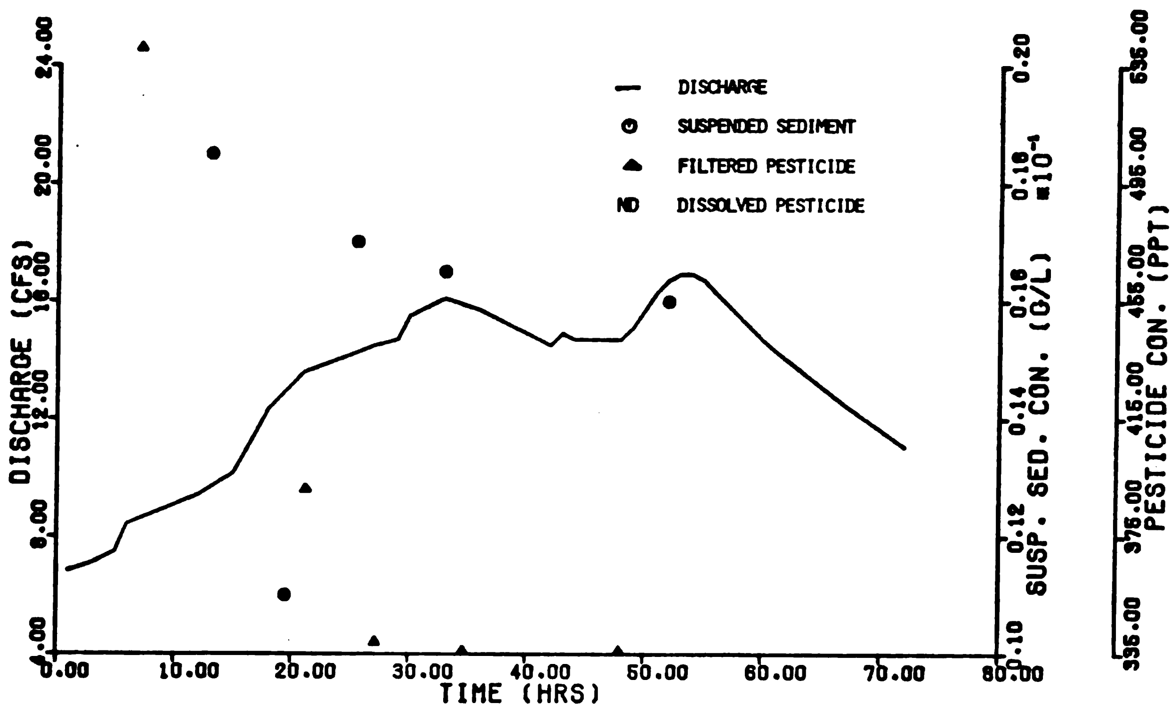

Figure 32.

DISCHARGE-SUSPENDED SEDIMENT-DDE RELATIONSHIP
FOR THE EVENT BEGINNING MAY 29, 1976

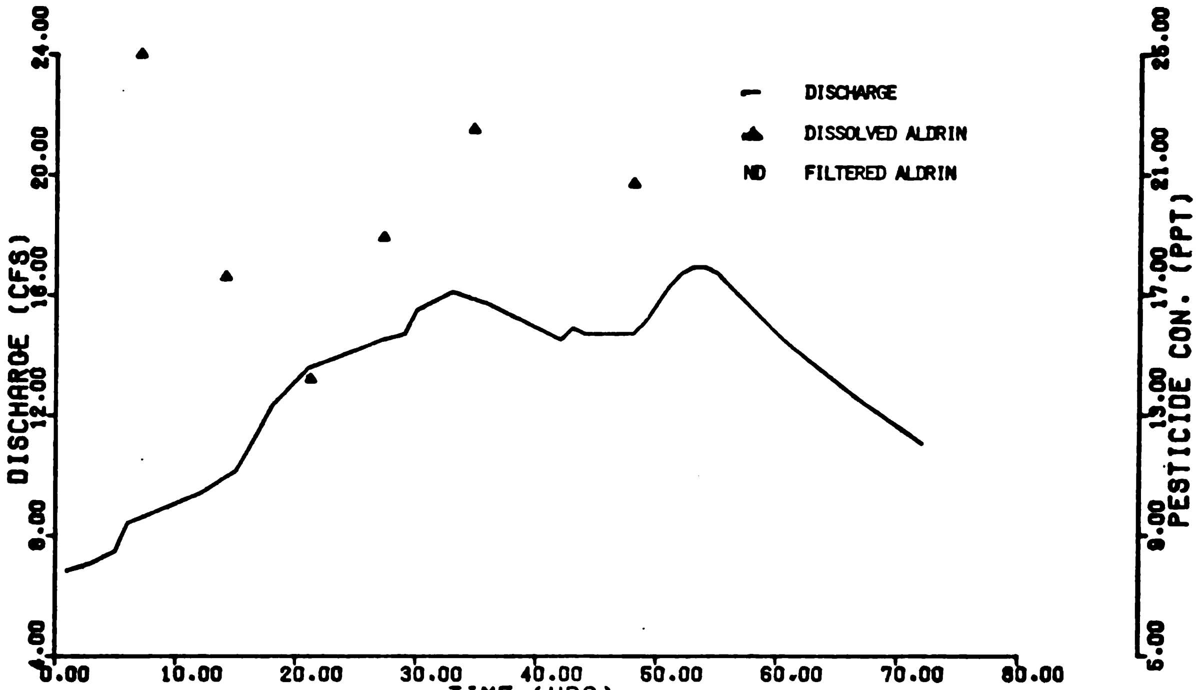

Figure 33.

DISCHARGE-PESTICIDE RELATIONSHIP

FOR THE EVENT BEGINNING MAY 29, 1976

p,p'DDT. The dissolved DDE was not detectable. Filtered Aldrin was not detectable, but the dissolved concentration was present and varied considerably. Little explanation can be offered other than the possible localized use of this pesticide in the past. With localized use, the pesticide enters the stream when the surface runoff is draining that area and may show up at a station downstream as a local peak in the time trace. The local peak may recede slowly, in the case of a plug load in which the pesticide continues to enter the surface runoff throughout the event, or it may recede quickly, in the case of a wash-out of the contaminated area by surface runoff. Dieldrin, Lindane and H. Epoxide were not detectable during this hydrograph.

Figures 34 and 35 show the time traces for the June 30, 1976 hydrograph. This is again relatively low flow. The suspended sediment is established immediately and decreases during the event, although not smoothly. The filtered p,p'DDT trace is stable at the beginning, but varies unreasonably during the recession of the hydrograph. The dissolved concentration shows some correlation with discharge, but is not real definitive. Other measurable pesticides were filtered Lindane and filtered DDE. The filtered DDE is an anticipated trace in relation to the discharge, but does not show a correlation to the suspended sediment. The concentration level of DDE is quite small, a maximum of 6 ppt. The dissolved concentration of DDE was not detectable. The filtered Lindane appears to be inversely proportional to both discharge and suspended sediment in this time trace, an occurrence which is unreasonable. This suggests that the data may be in error, since any possible explanation would involve a localized or extraordinary effect not characteristic of the watershed or pesticide.

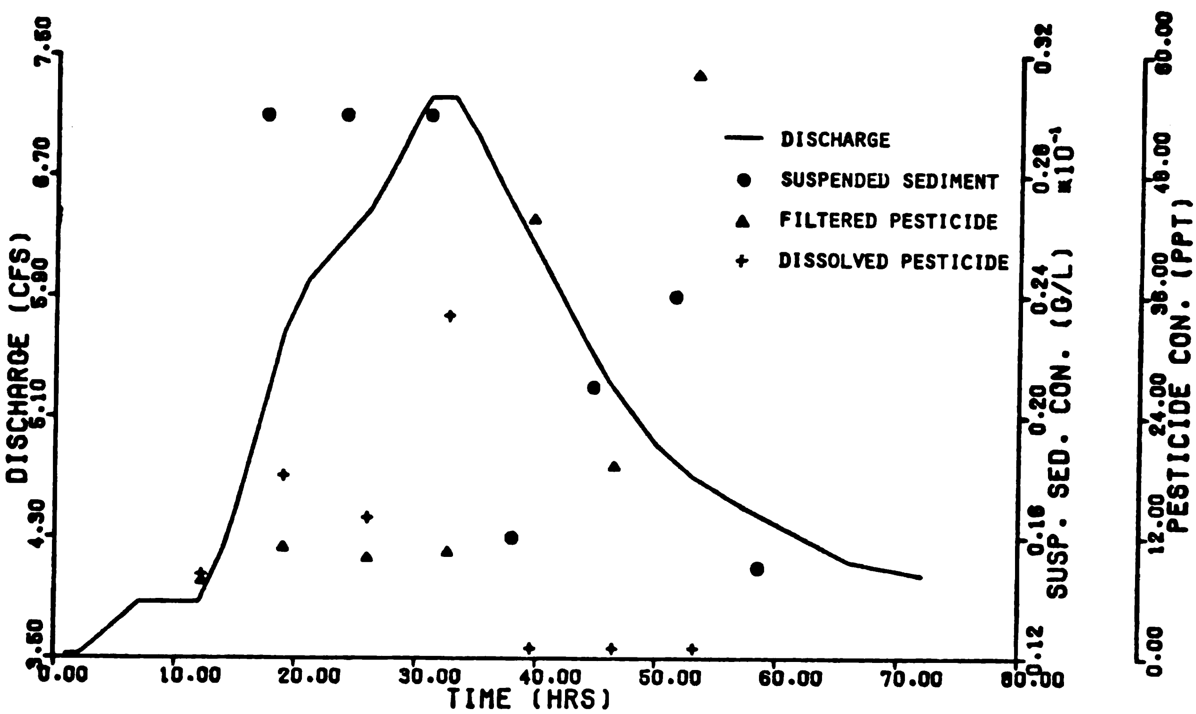

Figure 34.

DISCHARGE-SUSPENDED SEDIMENT-DDT RELATIONSHIP
FOR THE EVENT BEGINNING JUNE 30, 1976

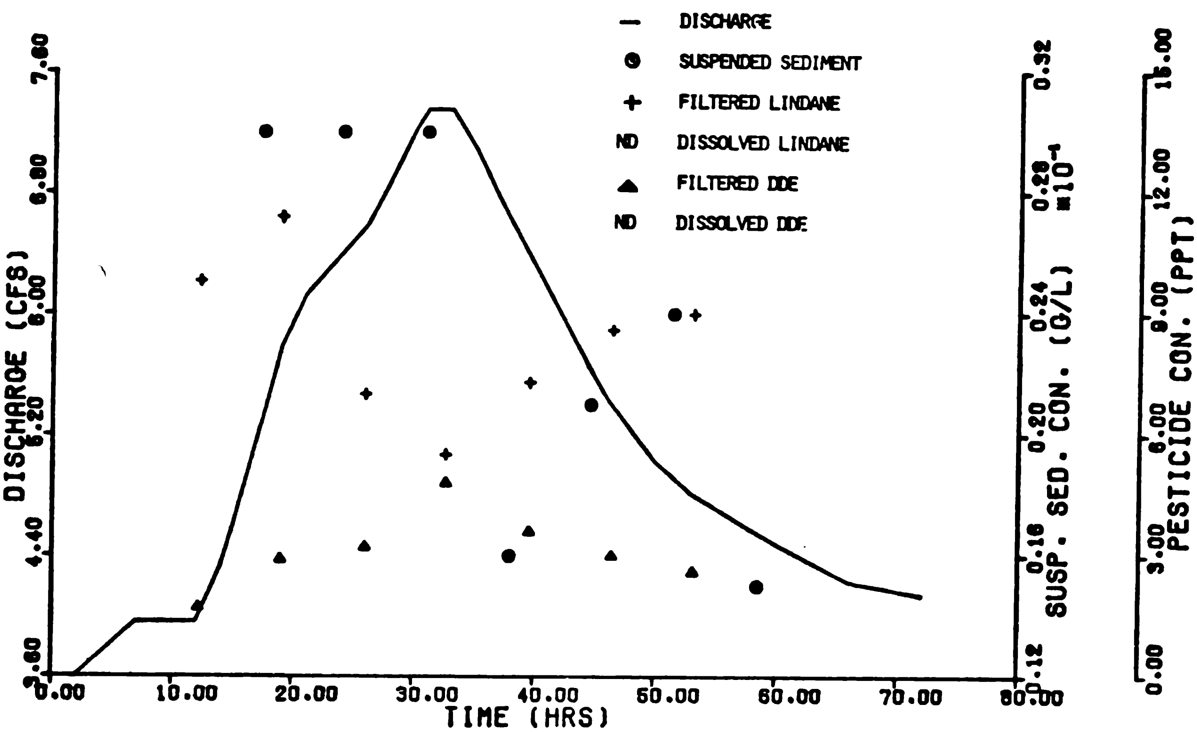

Figure 35.

DISCHARGE-SUSPENDED SEDIMENT-PESTICIDE RELATIONSHIP

FOR THE EVENT BEGINNING JUNE 30, 1976

6.2.2 Comparison of Time Traces

The June 17, 1975 and May 6, 1976 hydrographs (Figures 20 and 30) produce a consistent shape for the pesticide time trace. It is apparent that the dissolved pesticide concentration is strongly correlated with stream discharge and the adsorbed concentration appears quite dependent on suspended sediment. Figures 24 and 30 show the dissolved pesticide traces for the June 17, 1975 and May 6, 1976 events, respectively. The dissolved concentration of p,p'DDT, Dieldrin and Aldrin increase from the latter event to the former as expected due to the increase in stream discharge. Though the correlation is apparent in both events, the traces for May 6, 1976, decrease more rapidly. The adsorbed concentration traces (Figures 23 and 29) are similar in shape, but the difference in concentration levels between the two years is disturbing. The adsorbed concentrations for p,p'DDT on June 30, 1975, vary from 1 to 40 ppb while the concentrations for May 6, 1975, are in the range of 1 to 50 ppt. The possibility of pesticide degradation of this magnitude on the soil does not agree with other reports (Schacht, 1974), in which adsorbed levels in the part per billion range were recorded consistently. The inconsistency in concentration levels is balanced by the similarity in the trace form. Figure 29 shows the p,p'DDT and DDE levels decreasing at about the same rate as the suspended sediment. The only remaining explanation for the drop in concentration adsorbed on sediment is the contaminated soil is being washed-out of the watershed.

The smaller events of May 20 and June 30, 1976, are difficult to compare to the larger hydrographs already discussed because of the dominance of localized effects. For small storms and storms of low intensity, long duration rainfall, the runoff is a minimum resulting from reduced sheet flow and erosion. As a result, the suspended sediment concentration is quickly established and generally begins decreasing early due to the low wash load. Also, localized storms in the watershed cause variations in the time trace which may appear as local peaks. These two events appear to establish a maximum concentration quickly. The p,p'DDT is relatively stable in both cases, although during the recession of the June 30 hydrograph, considerable fluctuation is experienced. The high concentration of filtered DDE recorded on May 29 is difficult to explain in that during the May 6 hydrograph a maximum of 44 ppt occurred. On May 29, the concentration increased to over 500 ppt and on June 30, the filtered concentration was down to 5 ppt. The origin of a large dosage of DDE is unexplainable except for the possibility of pesticide dumping or container washing.

The concentration time traces during low flow conditions are affected by localized effects. Under these conditions, sediment and pesticide trace are not consistent and correlation cannot be expected. For high flow situations, it appears that when enough data is available, a definitive relationship for chlorinated hydrocarbon pesticide loss may be possible.

CHAPTER 7

DISCUSSION, CONCLUSIONS, AND RECOMMENDATIONS

Any interpretation of the nature of the transport mechanism from the results presented in this and the previous chapter should be regarded as speculative since the data is from three events of 1976, in which the high flow data reflects measurements taken during the recession of the hydrograph.

From the results of the sediment and pesticide concentration data, it is apparent that a correlation between the pesticide concentration (both adsorbed and dissolved) and stream discharge is much more likely for high flow conditions than for low flow conditions. Figure 36 and 37 show the concentration of adsorbed and dissolved p,p'DDT plotted versus the stream discharge for the 1976 data available. The possibility of a relationship between stream discharge and concentration is apparent for stream discharge greater than 20 cfs. However, for flows below 20 cfs the concentration of both adsorbed and dissolved p,p'DDT is quite variable. In this zone, the maximum as well as the minimum concentrations were measured. A similar behavior is exhibited by the other chlorinated hydrocarbons and the suspended sediment; however, more data will be required before this can be conclusively stated. This phenomenon suggests that there are different transport mechanism operating in these flow regions. The scatter of data points for flows less than 20 cfs cannot be explained by the hysteresis effect alone, but may in part be

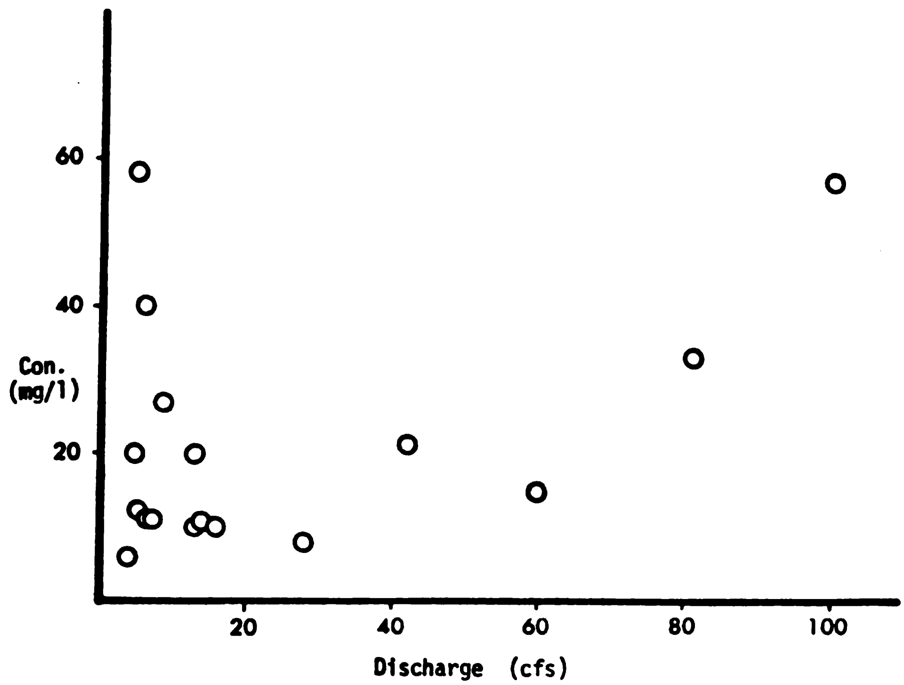

Figure 36. Adsorbed p,p'DDT - Discharge Relationship

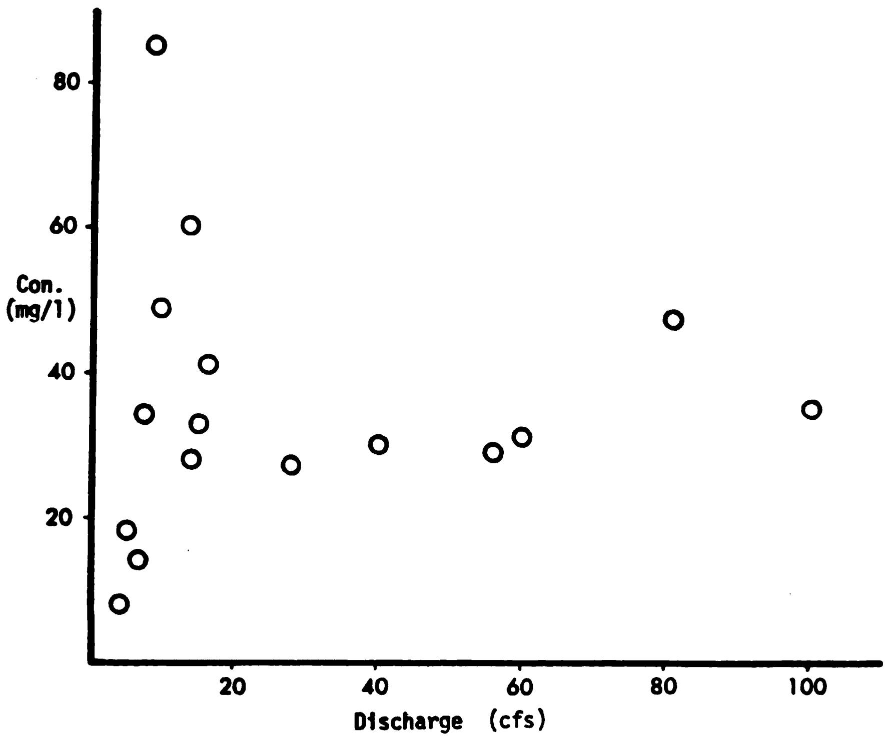

Figure 37. Dissolved p,p'DDT - Discharge Relationship

attributed to the origin and initiation of particle movement in the watershed.

Rainfall initiates soil particle motion by erosion and sheet flow. Some of these particles may enter the stream as wash load while others are deposited overland and in gullies - awaiting the occurrence of another storm to complete their journey to the stream. The variety of farming practices in the watershed, i.e., plowing and the application of pesticide, the topography of the area and the nonuniformity of rainfall intensity all contribute to the character of the wash load entering the stream. Hence, the soil particles contributed by the wash load enter the stream at varying times and locations and, therefore, will not necessarily be correlated with surface runoff regardless of a uniform rainfall distribution. The sediment contribution due to the wash load increases during the initial stages of overland flow and peaks soon after the storm subsides. At the time the stream flow is at the peak discharge, approximately 12 hours after the storm for Mill Creek, the wash load has diminished considerably. However, entrainment of bed material is possible at this time and the bed becomes a significant source of sediment for high flows. The entrained bed material may be the major contribution to the suspended sediment present in the stream at high flows because (1) the scouring action is much more effective for the high flows experienced at the peak of the hydrograph and (2) the fact that at this stage of the hydrograph the wash load is minimal. The hydrodynamic forces acting on the bed particles are directly proportional to the flow as shown in Chapter 5 and, therefore, the concentration of suspended sediment resulting from the entrainment of bed material will be correlated with discharge. Figure 38 shows schematically the sediment

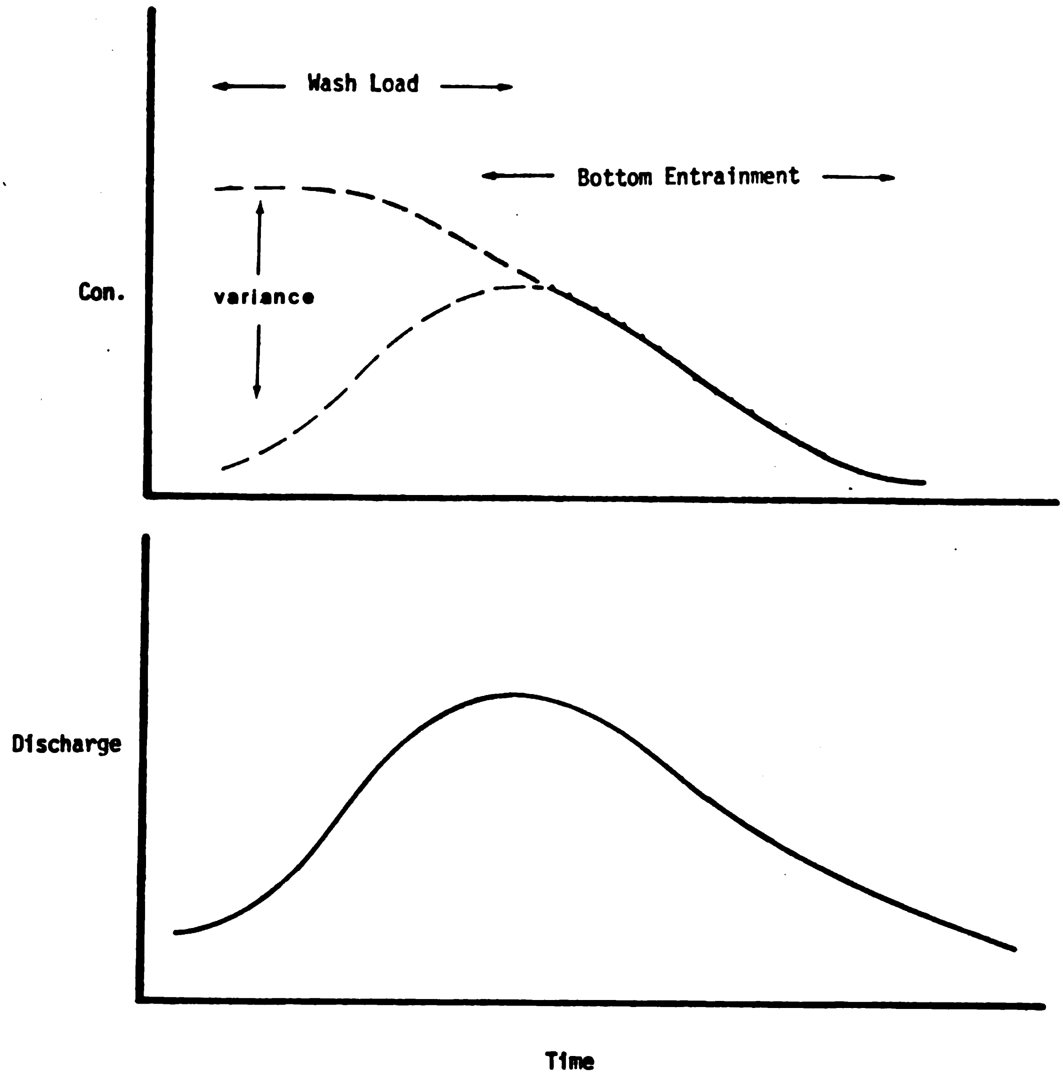

Figure 38. Suspended Sediment Concentration - Discharge Relationship

concentration and stream discharge for a hydrograph and the intervals where wash load and bottom entrainment are significant.

Pesticide laden particles are not uniformly distributed throughout the watershed due to its application which is dependent on land use. It is not necessarily true that a location of high erosion has been exposed to pesticides. Even for uniformly distributed rainfall, the contribution of pesticides from the wash load may be quite variable with no apparent correlation to sediment concentration. However, if the bed is contaminated with pesticides, the channel bottom becomes a source for pesticide transport which may be correlated with flow when the wash load contribution is small. Contamination of the bed may occur as a result of (1) desorption of pesticide from particles which have settled to the bottom and (2) adsorption of pesticide on the bed material from the dissolved concentration in the flow.

Superimposed on the fluctuating sediment concentration due to the nature of the wash load, the pesticide concentration time trace can be expected to be quite variable. However, for the case of a contaminated bed and high flows (when bed particle entrainment is the major source of sediment), a correlation of pesticide concentration with stream discharge or suspended sediment may be anticipated.

There are two mechanisms responsible for the presence of dissolved pesticide in the stream: (1) desorption from sediment particles and (2) mechanical scrubbing of the particle surface. Significant desorption of p,p'DDT can occur in a matter of hours (Wolcott, 1977). As a result, the contaminated wash load and suspended bed material can impart dissolved pesticide into the flow at a relatively fast rate. In addition, the mechanical scrubbing action caused by turbulence further enhances the dissolved concentration. However, dissolved and adsorbed pesticide may not always be detectable for all the chlorinated hydrocarbons because of their varying sorption rates and the dependence of adsorbed pesticide concentration on sediment transport.

The flow condition at station 5 is hydraulically smooth for base flow. As the stream discharge increases during surface runoff, the time average viscous boundary layer decreases. As long as the hydraulically smooth condition is maintained, the time average lift force is toward the bed and, thus, inhibiting particle entrainment (Coleman, 1967). At a stream discharge of 20 cfs, the viscous boundary layer is approximately 0.4 millimeters thick (Appendix B). This corresponds to the diameter of large sand particles found in the bed. That is, at a stream discharge of approximately 20 cfs, the viscous boundary layer at station 5 is penetrated by large sand particles and the bed becomes hydraulically rough. The gradient of the bed steepens and the roughness increases at station 26, but the flow condition between these two stations is essentially the same as that for station 5. As a result of the hydraulically rough condition, the time average lift force due to the pressure gradient is acting to promote entrainment over a major portion of the stream bed. From a hydrodynamic standpoint, it appears that for a hydraulically rough flow when the wash load is insignificant, a correlation between stream discharge and pesticide concentration is likely to be achieved, while for the hydraulically smooth case, any correlation between stream discharge and concentration seems remote.

From the suspended sediment and pesticide concentrations measured, it may be concluded that for sediment and pesticide transport:

1. A correlation between pesticide concentration (both adsorbed

and dissolved) and stream discharge may be possible for the hydraulically rough condition while the possibility is remote for the hydraulically smooth condition.

2. A correlation may not necessarily exist between suspended sediment and chlorinated hydrocarbon pesticides.
3. The seepage force is significant compared to other forces in the resultant force concept. However, in areas where the bed is fluidized and piping occurs, the flow condition resembles a turbulent jet and the resultant force concept cannot be applied.

The results of the sediment and pesticide transport study indicate that additional data on high flow surface runoff events is required. Data acquisition is continuing and additional information should be available in the future. From the results obtained for suspended sediment, it is recommended that the sampling procedure be altered so that several samples are taken in the vertical. In this way a more representative sample for pesticide analysis and suspended sediment load may be obtained.

If several high flow events can be monitored, the following work may prove significant:

1. Analysis of the chlorinated hydrocarbon pesticides for definitive relationships characteristic of the pesticide and watershed involving sediment, pesticide, and stream discharge.
2. Analysis of stream bed samples to determine the degree of pesticide contamination. This would provide evidence to substantiate the pesticide transport theory and its dependence on the hydraulic nature of the bed.
3. Evaluate the sorption process between sediment and the pesticides

considered so that a better understanding of the relationship between dissolved and adsorbed pesticide is obtained.

4. Analysis of the precipitation distribution and possible accompanying localized runoff to identify areas that are a significant pesticide source.

LIST OF REFERENCES

LIST OF REFERENCES

Aksoy, S. 1973. Fluid Force Acting on a Sphere Near a Solid Boundary. Proceedings of 15th International Association for Hydraulic Research Congress, Istanbul, Turkey, A29.

Apperley, L. W. 1968. Effect of Turbulence on Sediment Entrainment. Ph.D. Thesis, University of Auckland, Auckland, New Zealand.

Barthel, W. F. 1966. Surface Hydrology and Pesticides. Pesticides and Their Effects on Soils and Water, Special. Pub. No. 8, Soil Science Soc. Amer., Inc.

Berck, B. 1953. Microdetermination of DDT in River Water and Suspended Soils. Anal. Chem. 25:1253-1256.

Brodkey, R. S. 1977. Stereoscopic Visualization of Turbulent Shear Flows. Seminar, Michigan State University.

Brahms, A. 1753. Anfangsgrunde der Deich-n-Wesserbaukunst.

Chepil, W. S. 1959. Equilibrium of Soil Grains at the Threshold of Movement by Wind. Proceedings, Soil Science Society of America. Vol. 23, Madison, Wisc.

Chen, C. N. and M. R. Carstens. 1973. Mechanic of Removal of a Spherical Particle From a Flat Bed. Proceedings of 15th International Association for Hydraulic Research Congress, Istanbul, Turkey, A30.

Clark, D. R. 1965. The Effects of Seepage on the Dynamic Forces on Hemispheres at the Surface of a Permeable Bed of a Flowing Channel. Master Thesis, Utah State University, Logan, Utah.

Clayton, L., S. J. Tuthill, and W. B. Bickley. 1966. Effects of Groundwater Seepage on the Regimen of an Alaskan Stream. 47th Annual Meeting of American Geophysical Union, Washington, D.C.

Colby, B. R. 1957. Relationship of Unmeasured Sediment Discharge to Mean Velocity. Transactions, American Geophysical Union, Vol. 38, No. 5.

Coleman, N. L. 1967. A Theoretical and Experimental Study of Drag and Lift Forces Acting on a Sphere Resting on a Hypothetical Streambed. Proceedings of the 12th International Association for Hydraulic Research Congress, Fort Collins, C22.

Donigan, A. S. and N. H. Crawford. 1976. Moedling Pesticides and Nutrients on Agricultural Lands. EPA Report 600/2-76-043.

Egiazaroff, I. V. 1957. L'Equation generale du transport des alluvions non cohesives par un courent fluide. Proceedings of the 7th Congress, International Association for Hydraulic Research, Lisbon, Portugal, D43.

Einstein, H. A. and E. A. El-Samni. 1949. Hydrodynamic Forces on a Rough Wall. Reviews of Modern Physics, Vol. 21, No. 3.

Einstein, H. A. and H. Li. 1958. The Viscous Sublayer Along a Smooth Boundary. Transactions, ASCE, Vol. 123, No. 2992.

Felton Herron Creek, Mill Creek Pilot Watershed Studies. 1974. Work Plan. Institute of Water Research, Michigan State University.

Fortier, S. and F. C. Scobey. 1926. Permissible Canal Velocities. Transactions, ASCE, Vol. 89, No. 1588.

Garde, R. J. and S. Sethuraman. 1969. Variation of the Drag Coefficient of a Sphere Rolling Along a Boundary. La Hoville Blanche, No. 7.

Gessler, J. 1965. The Beginning of Bed Load Movement of Mixtures Investigated as Natural Armoring in Channels. Lab of Hydraulic Research, Swiss Federal Institute of Technology, Zurich, No. 69.

Gillett, J. W., J. Hill, A. W. Jarvinen, and W. P. Schoor. 1974. A Conceptual Model for the Movement of Pesticides Through the Environment. EPA-660/3-74-024.

Harrison, S. S. 1968. The Effects of Groundwater on a Stream Regimen - A Laboratory Study. Ph.D. Dissertation, University of North Dakota.

Ippen, A. T. 1953. The Motion of Discrete Particles Along the Bed of a Turbulent Stream. Proceedings, Minnesota International Hydraulics Conference.

Jeffreys, H. 1929. Transport of Sediment by Streams. Proceedings, Cambridge Philosophical Society, Vol. 25.

Kalinske, A. A. 1942. Criteria for Determining Sand Transportation by Surface Creep and Saltation. Transactions, American Geophysical Union.

Kalinske, A. A. 1947. Movement of Sediment as Bed Load in Rivers. Transactions, American Geophysical Union, Vol. 28, No. 4.

Kramer, H. 1935. Sand Mixtures and Sand Movement in Fluvial Models. Transactions, ASCE, Vol. 100, No. 1909.

Krey, H. 1927. Die Quergeschwindigkeitskurve bei Turbulenter Stroemung. Zeitschrift for Angewandte Mathematik and Mechanik, Vol. 7, No. 2.

Lane, E. W. 1955. Design of Stable Channels. Transactions, ASCE, Vol. 120, No. 2776.

Lyles, L. 1972. Boundary Layer Flow Structure: Effects on Detachment of Noncohesive Particles. Sedimentation, Colorado State University.

Martin, C. S. 1970. Effect of Pourous Sand Bed on Incipient Sediment Motion. Water Resources Research, Vol. 6, No. 4.

Martin, C. S. 1971. Seepage Force on Interfacial Bed Particles. Proceedings, ASCE, Vol. 97, No. HY7.

McNown, J. S. 1948. Influence of the Boundary Proximetry on the Drag of Spheres. Proceedings at 7th International Congress of Applied Mechanics, London.

Mavis, F. T. and L. M. Laushey. 1949. Formula for Velocity at Beginning of Bed Load Movement is Reappraised. Civil Engineering, ASCE, Vol. 19, No. 1.

Meyer-Peter, E. and R. Muller. 1948. Formulas for Bed Load Transport. Report on 2nd Meeting of International Association for Hydraulic Resea ch, Stockholm.

Raudkivi, A. J. 1963. Study of Sediment Ripple Formation. Journal of the Hydraulics Division, ASCE, Vol. 89, HY6.

Reitz, W. 1936. Uber Geschiebebewegung. Wasserwirtsch and Tech., No. 28.

Rubey, W. W. 1948. The Forces Required to Move Particles on a Stream Bed. Professional Paper 189 B, USGS.

Sanborn, J. R. 1974. The Fate of Selected Pesticides in the Aquatic Environment. EPA Report 660/3-74-025.

Schoklitsch, A. 1914. Uber Schleppkraft and Geschiebebewegung. Engelmann, Leipzig.

Sckacht, R. A. 1974. Pesticides in the Illinois Waters of Lake Michigan. EPA Report 660/3-74-002.

Sedimentation Engineering, 1975. ASCE-Manuals and Reports on Engineering Practice - No. 54.

Shields, A. 1936. Anwendung der Ahnlichkeitsmechanik and Turbulenz forschung aut die Geschiebebewegung, Berlin.

Shin, Y. 1970. Adsorption of DDT by Soils and Biological Materials. Ph.D. Thesis, Michigan State University.

Smith, G. E. 1974. Losses of Fertilizers and Pesticides from Claypan Soils. EPA Report 660/2-74-068.

Standard Methods, 1971. American Public Health Association, Washington, D.C.

Sternberg, H. 1875. Untersuchungen uber das Langen und Querprofil geschiebefuhrender Flusse, Z. Bauwesen, Vol. 25.

Sutherland, A. J. 1967. Proposed Mechanism for Sediment Entrainment by Turbulent Flow, Journal of Geophysical Research, Vol. 72, No. 24.

Tarimcioglu, T. 1973. Determination of the Critical Condition on Mobile Beds in Open Channels. Proceedings of 15th International Association for Hydraulic Research, Istanbul, Turkey, A31.

Tisen, L. J. 1953. Recherchs sur la Tenison limite d'Entrainment des Materiaux constitutifs du Lit, Proceedings of 5th International Association for Hydraulic Research Congress, Minneapolis.

Todd, D. K. 1959. Groundwater Hydrology. John Wiley and Sons, Inc., New York, New York.

Watters, G. Z. and M. V. P. Rao. 1971. Hydrodynamic Effects of Seepage on Bed Particles. Journal of Hydraulics Division, ASCE, Vol. 97, HY3.

White, C. M. 1940. The Equilibrium of Grains on the Bed of a Stream. Proceedings of Royal Society of London, Vol. 174A.

Wolcott. 1977. Personal Communication at Michigan State University.

Yalin, M. S. 1963. An Expression for Bed Load Transportation. Proceedings of American Society of Civil Engineering, Vol. 91, No. HY2.

Yalin, M. S. 1972. Mechanics of Sediment Transport. Pergamon Press, New York.

Zandi, R. A. 1970. Advances in Solid-Liquid Flow in Pipes and Its Application. Pergamon Press, New York.

APPENDICES

APPENDIX A

APPENDIX A

APPLICATION OF THE INCIPIENT MOTION CRITERION

The conventional incipient motion criterion may be used for areas with normal seepage rates. This will be assumed applicable for that portion of the bed not under piping effects. The incipient motion (equation 12) is developed from consideration of the entraining and resisting forces. By calculating the effect of each of these forces, the significance of each can be established. The results will give an angle of repose which can be compared with that measured.

The forces parallel to the bed include the drag and the bouyant weight component. The forces perpendicular to the bed are the hydrodynamic lift, the shear lift, the bouyant weight component, and the seepage force. Table 10 defines the variables required to calculate these forces.

The velocities required for the lift and drag are very important quantities and difficult to obtain. The logarithmic velocity distribution is assumed to hold for a rough boundary:

$$\frac{u}{u_*} = 8.5 + 5.75 \log \left(\frac{y}{k_s}\right)$$

where k_s is the roughness height (in the range of the particle diameter), u is the velocity at height y, and u_* is the shear velocity. The lift equation requires the velocity at .35d above the bed and the drag requires the velocity at the top of the particle. The location of zero bed level, the origin from which y is measured, has been determined by investigators to be between .15d and .2d below the top surface of the sphere for uniform grain size. The location of the bed level is chosen as .2d.

The forces on a bed particle as defined in section 5.1 and estimated for the flow condition at station 5 are:

(a) Bouyant weight,

$$W_B = \frac{\pi}{6}(\gamma_s - \gamma)d^3 = 5.7\text{x}10^{-11} \text{ lb.}$$

(b) Total drag,

$$F_D = C_D\ \xi\ A_C\ \rho\frac{\overline{U}_T^{\,2}}{2} = 1.3\text{x}10^{-11} \text{ lb.}$$

(c) Hydrodynamic lift,

$$F_L = A_C\ C_L\ \rho\frac{\overline{U}_{35}^{\,2}}{2} = 3.6\text{x}10^{-12} \text{ lb.}$$

(d) Shear lift,

$$F_{SL} = \frac{\pi d^2}{8}\ \mu\ \frac{\partial V}{\partial y} = 1.9\text{x}10^{-13} \text{ lb.}$$

(e) Seepage force,

$$F_S = C(1+e)\gamma\ \frac{\partial h}{\partial y}\ \frac{\pi d^3}{6} = 1.7\text{x}10^{-11} \text{ lb.}$$

where A_C was assumed equal to the cross-sectional area of the upper .2d of the sphere and $\partial V/\partial y$ was calculated using the gradient obtained from the velocity at the top of the sphere. By dividing the force parallel to the bed (assuming a horizontal bed, $\alpha = 0$) by the forces perpendicular to the bed, the angle of repose was found to be 20 degrees.

Table 10. Incipient Motion Equation Variables.

Symbol	Parameter	Value	Definition
ρ	fluid density	1.94 slugs/ft^3	constant
γ	fluid specific weight	62.4 lb/ft^3	constant
K	von Karmons constant	0.4	constant
C	flow coefficient	0.37	experimentally determined by Martin (1970)
ξ	momentum correction coefficient	0.79	experimentally determined by Chen & Carstens (1973)
γ_s	particle specific weight	165 lb/ft^3	estimated
e	bed porosity	.2	estimated
α	bed slope	.0001	estimated
S_y	water surface slope	.0001	assumed equal to bed slope
C_D	drag coefficient	1.5	Eagleson (1959)
C_L	lift coefficient	.178	Einstein and El Somoni (1949)
U_*	shear velocity	.04	estimated
$\overline{U}_{35}$	velocity at .35d from bottom	.08 fps	logarithmic velocity equation
$\overline{U}_T$	velocity at top of sphere	.06 fps	logarithmic velocity equation
$\partial h/\partial y$	piezometric head gradient	.3	estimated

APPENDIX B

APPENDIX B

SUBLAYER DETERMINATION

The height of the time average viscous sublayer, δ, can be determined by the following relationship:

$$\delta = \frac{11.6}{u_*} \nu$$

The shear velocity, u_*, is a function of the velocity and is estimated to be one-tenth of the mean velocity. Figure 39 shows the relationship for velocity and stream discharge at station 5. For a stream discharge of 20 cfs, the mean velocity is approximately 0.8 fps. Therefore, the shear velocity is assumed to be 0.08 fps. The kinematic viscosity for water at 75°F is .00001 sq.ft. per second. This results in a sublayer of .00145 feet or .4 millimeters.

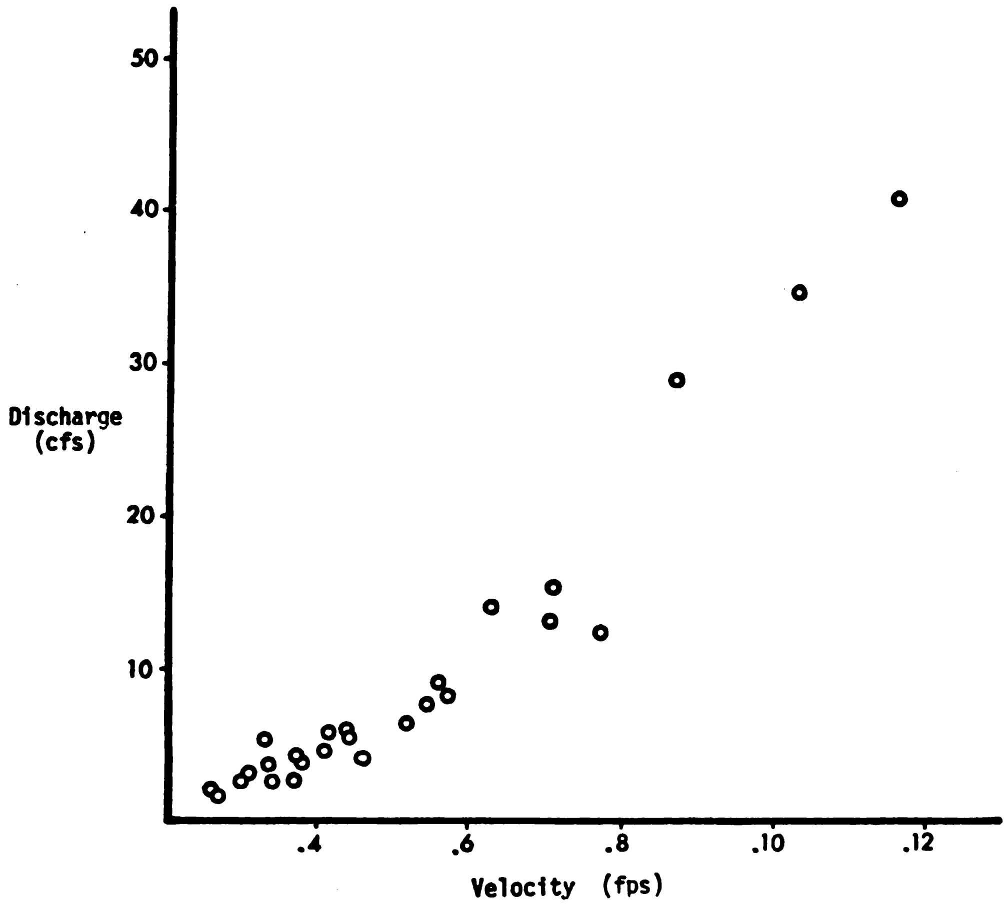

Figure 39. Discharge - Velocity Relationship - Station 5